GIScience & Remote Sensing

ISSN: 1548-1603 (Print) 1943-7226 (Online) Journal homepage: www.tandfonline.com/journals/tgrs20

Recent advances in TROPOMI-based methane source detection: a systematic review

Ruoqi Liu, Siqi Li , Geli Zhang , Mengyao Liu , Xiao Lu , Shushi Peng , Lu Shen , Yuzhong Zhang , Minghao Zhuang , Xiaoxing Zuo & Jinwei Dong

To cite this article: Ruoqi Liu, Siqi Li , Geli Zhang , Mengyao Liu , Xiao Lu , Shushi Peng , Lu Shen , Yuzhong Zhang , Minghao Zhuang , Xiaoxing Zuo & Jinwei Dong (2026) Recent advances in TROPOMI-based methane source detection: a systematic review, GIScience & Remote Sensing, 63:1, 2650822, DOI: 10.1080/15481603.2026.2650822

To link to this article: https://doi.org/10.1080/15481603.2026.2650822

GISCIENCE & REMOTE SENSING
2026, VOL. 63, NO. 1, 2650822
https://doi.org/10.1080/15481603.2026.2650822

Taylor & Francis by informa

REVIEW ARTICLE

OPEN ACCESS Check for updates

Recent advances in TROPOMI-based methane source detection: a systematic review

Ruoqi Liu[a], Siqi Li[a], Geli Zhang[a], Mengyao Liu[b], Xiao Lu[c], Shushi Peng[d], Lu Shen[e], Yuzhong Zhang[f], Minghao Zhuang[g], Xiaoxing Zuo[b,h] and Jinwei Dong[i]

[a]Department of Land Resources, College of Land Science and Technology, China Agricultural University, Beijing, China; [b]R&D Satellite Observations, KNMI, Royal Netherlands Meteorological Institute, De Bilt, The Netherlands; [c]Department of Atmospheric Physics and Chemistry, School of Atmospheric Sciences, Sun Yat-sen University, Zhuhai, China; [d]Department of Physical Geography and Natural Resources, College of Urban and Environmental Sciences, Peking University, Beijing, China; [e]Department of Atmospheric and Oceanic Sciences, School of Physics, Peking University, Beijing, China; [f]Key Laboratory of Coastal Environment and Resources of Zhejiang Province, School of Engineering, Westlake University, Hangzhou, China; [g]Department of Plant Nutrition, State Key Laboratory of Nutrient Use and Management, College of Resources and Environmental Sciences, Key Laboratory of Plant-Soil Interactions, Ministry of Education, China Agricultural University, Beijing, China; [h]Department of Geoscience & Remote Sensing, Delft University of Technology (TUD), Delft, The Netherlands; [i]Key Laboratory for Resource Use and Environmental Remediation, Institute of Geographic Sciences and Natural Resources Research, Chinese Academy of Sciences, Beijing, China

ABSTRACT

The renewed increase in atmospheric methane (CH_4) concentrations since 2007, culminating in record growth rates in 2021, poses a critical challenge to achieving global climate targets. The TROPOspheric Monitoring Instrument (TROPOMI) onboard the Sentinel-5 Precursor satellite provides unprecedented daily global observations of CH_4 at a spatial resolution ($7 \times 7\ km^2$, improved to $5.5 \times 7\ km^2$ since August 2019), enabling substantial advances in space-based CH_4 monitoring and emission quantification. Here, we synthesize and categorize 133 published studies spanning global, regional and local scales and covering both anthropogenic and natural CH_4 sources. Collectively, these studies demonstrate TROPOMI's capability to quantify emissions across diverse spatiotemporal scales, as well as its synergy with other satellite instruments for detecting and attributing facility-level sources, such as fossil fuel infrastructure and landfills. However, emission estimates remain challenged by uncertainties in column-averaged CH4 (XCH_4) retrievals related to surface albedo effects and persistent cloud cover, particularly in tropical and high-latitude regions. These limitations can be mitigated through improved retrieval algorithms, refined quality filtering, multisatellite fusion, and integration with ground-based observations and airborne campaigns. Furthermore, we assess the suitability of different quantification approaches for specific source types, such as Gaussian plume models for large isolated emitters and inverse modeling for spatially diffuse emissions. Finally, we outline key methodological priorities and opportunities in the context of the recent MetOp-SG-A satellite, which will complement TROPOMI with a morning overpass. By consolidating current applications of TROPOMI XCH_4 observations, this review provides guidance for enhancing space-based methane monitoring and supports targeted mitigation strategies aligned with achieving Sustainable Development Goal 13.

ARTICLE HISTORY
Received 15 August 2025
Accepted 21 March 2026

KEYWORDS
Methane (CH_4); TROPOMI; emission monitoring; source detection; atmospheric inversion

1. Introduction

Methane (CH_4) is the second most potent greenhouse gas, with a 20-year warming potential approximately 80 times greater than that of CO_2, and has accounted for about 20% of total greenhouse gas-related radiative forcing since the preindustrial era (IPCC 2023). Given that CH_4 has a relatively short atmospheric lifetime of 11.2 ± 1.3 years compared with CO_2, reducing CH_4 emissions is an effective strategy for mitigating near-term climate warming (Nisbet et al. 2019). However, atmospheric CH_4 concentrations have

CONTACT Geli Zhang geli.zhang@cau.edu.cn

Supplemental data for this article can be accessed online at https://doi.org/10.1080/15481603.2026.2650822.

increased rapidly again since 2014, and the causes remain uncertain (Nisbet et al. 2016). CH_4 emissions originate from both natural sources (~40%, including wetlands, termites, and wildfire) and anthropogenic sources (~60%, including fossil fuels, ruminants, agriculture, and waste) (Saunois et al. 2025). The primary sink for atmospheric CH_4 is oxidation by the hydroxyl radical (OH). Accurate observations of atmospheric CH_4 concentrations are therefore essential for attributing sources and sinks, which underpins targeted mitigation measures and projections of future climate change (European Commission and United States of America 2021; IPCC 2023).

Satellite remote sensing has become a critical tool for monitoring atmospheric CH_4 concentrations and quantifying CH_4 emissions across scales ranging from local to regional (Jacob et al. 2016). The Scanning Imaging Absorption Spectrometer for Atmospheric ChartographY (SCIAMACHY) was a pioneering instrument for CH_4 monitoring by first introducing nadir near-infrared (NIR) and shortwave-infrared (SWIR) solar reflectance, operating from 2002 to 2012 (Bloom et al. 2010; Hayashida et al. 2013). Subsequently, the Greenhouse Gases Observing Satellite (GOSAT) launched in 2009, has provided CH_4 observations with a spatial resolution of ~10.5 km-diameter discrete circular pixels (Barr et al. 2025; Lu et al. 2022). Recently, target satellite instruments with very high spatial resolution (<60 m) and detection thresholds of approximately 100–10,000 kg h^{-1} have been developed, including GHGSat, PRISMA, EnMAP, and Carbon Mapper. However, their coarse temporal coverage and data gaps limit their application primarily to detecting large individual sources at the local scale (Duren et al. 2025; Jervis et al. 2021; Nesme et al. 2021; Roger et al. 2024; Settembre et al. 2025). A major advance in CH_4 monitoring is the TROPOspheric Monitoring Instrument (TROPOMI) aboard the Sentinel-5 Precursor satellite, launched in October 2017. TROPOMI provides daily global observations of column-averaged atmospheric CH_4 (XCH_4) at a spatial resolution of 7×7 km^2 (refined to 5.5×7 km^2 since August 2019) (Hu et al. 2016, 2018; Lorente et al. 2021; Veefkind et al. 2012). Its high data coverage and advanced inversion techniques enable near real-time monitoring of CH_4 emissions from local to global scales.

TROPOMI observations have been widely applied to quantify CH_4 emissions from oil and natural gas production (de Gouw et al. 2020; Zhang et al. 2020), wetlands in Africa and South America (Li et al. 2024b; Pandey et al. 2021), and urban landfills (Maasakkers et al. 2022b), as well as sectoral emissions at national to global scales (Chen et al. 2022; Lu et al. 2022; Qu et al. 2021; Shen et al. 2021; Yu et al. 2023). These findings demonstrate that TROPOMI observations not only provide complementary capabilities to target satellites in identifying large emitters but also offer superior coverage for consistent regional- to global-scale monitoring.

While TROPOMI retrievals and applications have been continuously explored, existing studies of satellite-based CH_4 observing systems lack a dedicated and systematic review of the rapidly expanding body of TROPOMI-based CH_4 applications and findings (Liu and Wang, 2021b; Jacob et al. 2022; Jacob et al. 2016; Liu et al. 2022). In this study, we synthesize progress in research using TROPOMI XCH_4 data, identify key areas, and provide guidance for future development. Moreover, Sentinel-5, launched on August 13, 2025, as a successor to Sentinel-5P, will measure CH_4 concentration with a morning equator crossing time (~10:00 local time), complementary to TROPOMI's early afternoon overpass (~13:30). This enhanced temporal sampling will further strengthen satellite-based CH_4 monitoring. A consolidated assessment of TROPOMI applications is therefore timely and essential for both researchers and policymakers seeking to advance atmospheric CH_4 science and inform mitigation strategies.

This review is organized as follows. (1) We first introduce the major TROPOMI XCH_4 products and their characteristics; (2) we review TROPOMI-based CH_4 monitoring at global, regional, and local scales and categorize studies by source type, including fossil fuels, livestock, waste, rice paddies, and wetlands; and (3) we discuss current challenges and prospects for TROPOMI CH_4 observations within the evolving satellite observing system.

2. TROPOMI CH_4 concentration products

TROPOMI monitors atmospheric CH_4 through solar reflectance in the shortwave infrared (SWIR), enabling retrieval of column-averaged CH_4, provided that surface–atmosphere light paths are accurately characterized (Frankenberg, Platt, and Wagner 2005). Currently, three main TROPOMI XCH_4 products are summarized in Table 1.

Table 1. TROPOMI XCH_4 products.

Product	Product release frequency	Period	Retrieval algorithm	Version	Advantages	Limitations
OPER-OFFL	1 day	2018.04.30-present	RemoTeC (version-dependent differences)	v01.02.02-v01.04.00; v02.02.00-v02.03.01; v02.04.00-current version	Near real-time	System errors from different algorithms between versions; strict quality filter
OPER-RPRO	—[a]	2018.04.30-2022.07.25[b]	Optimal RemoTeC (uniform retrieval)	v02.04.00	Long-term data with a uniform algorithm	Strict quality filter
WFMD	~ 5 month	2017.11.01-~5 month before present	WFM-DOAS	v1.2, v1.5, v1.8, v2.0	Long-term data with a uniform algorithm; machine learning-based quality filter and bias correction	Limited physical interpretability of bias correction

[a] These full-period data product were released in July 2022.
[b] The optimal retrieval algorithm developed by Lorente et al. (2021) was used for operational offline data products after v02.04.00.

(1) The operational TROPOMI-S5P CH_4 product (OPER-OFFL) is released in near real time and retrieved using the RemoTeC full-physics algorithm (Butz et al. 2011; Hasekamp and Butz 2008; Hu et al. 2016). This algorithm simulates CH_4 absorption spectra via radiative transfer modeling combined with iterative optimization, with several updates implemented across successive product versions.
(2) The operational reprocessed TROPOMI-S5P CH_4 product (OPER-RPRO) provides a consistently reprocessed full data record using the RemoTeC algorithm, incorporating substantial improvements in both retrieval implementation (e.g. regularization and spectroscopy) and postprocessing (e.g. bias correction and quality filtering) (Lorente et al. 2023; Lorente et al. 2021).
(3) The TROPOMI WFM-DOAS XCH_4 data product (TROPOMI/WFMD) is derived from the WFM-DOAS algorithm, which applies a linear least-squares fit of precomputed weighting functions to the SWIR spectra. This method is less sensitive to errors in aerosol, albedo, and surface-reflectance modeling (Schneising et al. 2019; Schneising et al. 2023). The latest TROPOMI/WFMD v2.0 used more refined quality filtering based on an improved extreme gradient boosting (XGBoost) classifier and an expanded training dataset (Schneising et al. 2025).

TROPOMI/WFMD and operational data products show good overall agreement and are often used to cross-validate each other in applications and evaluation studies (Hachmeister et al. 2022; Karoff and Vara-Vela 2023; Lorente et al. 2021).

The operational and WFMD data exhibit distinct data coverage due to discrepancies in retrieval algorithms, quality filtering, and posterior bias corrections. These differences are particularly pronounced in regions with complex observation conditions, such as very low or high surface albedo (e.g. concrete, rock, or wetlands), extreme solar zenith angles, and strong aerosol scattering. The latest operational data mitigate residual albedo-related biases using a posteriori correction that is fully independent of reference data (Lorente et al. 2023; Lorente et al. 2021). However, nonconvergence remains a common issue in the full-physics algorithm, and the empirical threshold-based quality filtering removes a large number of observations in tropical and high-latitude areas. In contrast, the TROPOMI/WFMD product applies a nonlinear machine learning classifier incorporating VIIRS cloud data to rapidly identify low-quality scenes under simplified physical assumptions (e.g. cloud-free scenes). Its data-driven bias correction, based on XCH_4 climatology ($SLIMCH_4$) and environmental variables, better captures complex dependencies in the observations (Schneising et al. 2019; Schneising et al. 2023). As a result, the latest TROPOMI/WFMD v2.0 shows increased data coverage at mid and high latitudes (e.g. the Sahara, Central Europe, and Siberia) by more than 10%, with Arctic coverage improving by about 40% (Schneising et al. 2025). This product generalizes well to previously unseen data and achieves improved precision. Figure 1 shows the global annual average of XCH_4 in 2021 from the latest version of each product.

Validation of TROPOMI XCH_4 data is typically performed using reference measurements from ground-based networks (Sha et al. 2021), such as the Total Carbon Column Observing Network (TCCON) (Wunch et al. 2011). The quality of TROPOMI XCH_4 retrieval products has improved significantly with recent version updates. The latest validation report (v28.00.00, 15 September 2025) (Lambert et al. 2025) indicates that the operational TROPOMI XCH_4 column data (v02.04.00-current version, April 2018–August 2025) exhibit biases against the TCCON of −0.36% (standard) and +0.20% (bias-corrected). For the new TROPOMI/WFMD XCH_4 v2.0 product, the global bias relative to TCCON is reduced to 0.65 ppb, with a random error of 13.35 ppb and a total systematic error of 4.86 ppb (Schneising et al. 2025). The Collaborative Carbon Column Observing Network (COCCON) has also been used to validate different versions of operational TROPOMI XCH_4 data across regions in Russia (Alberti et al. 2022), Greece (Mermigkas et al. 2021), and Antarctica (Pollard et al. 2022). Furthermore, the portable Bruker EM27/SUN Fourier transform infrared spectrometer has been used for validation in East Africa (Jinja, Uganda) (Humpage et al. 2024), revealing a mean XCH_4 difference of −0.44% for the operational OFFL product (v01.03.02). Such a sensor significantly improved data reliability in complex urban environments (Park et al. 2024).

In practice, these TROPOMI XCH_4 products have been widely applied from local to global scales and covering both natural and anthropogenic sources (OPER: e.g. Chen et al. 2023; Lauvaux et al. 2022; Qu et al. 2021; Yu et al. 2023; WFMD: e.g. Schneising et al. 2020; Vanselow et al. 2024). Moreover, both OPER-RPRO and WFMD products employ a consistent retrieval algorithm throughout their full records and better

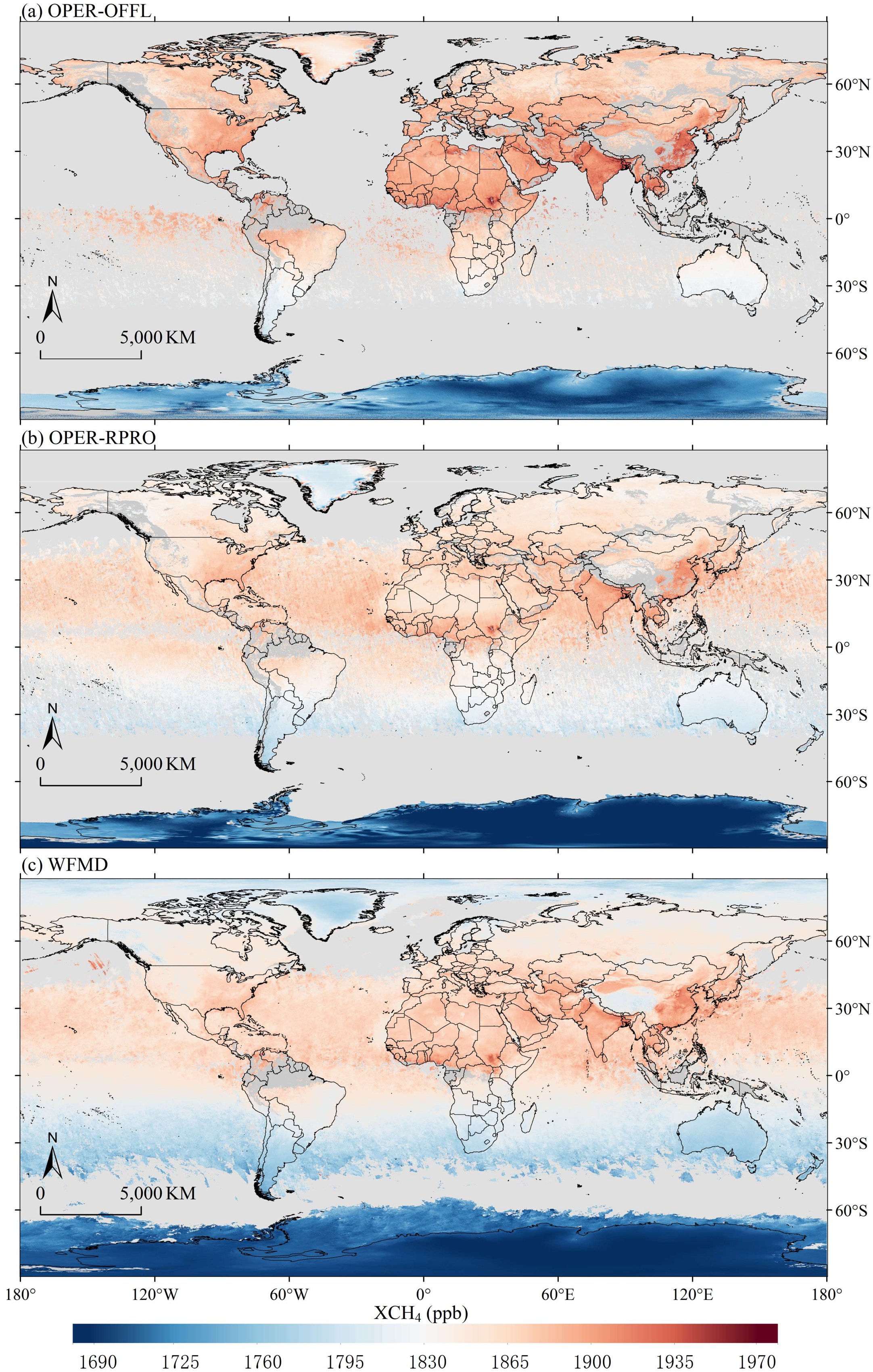

Figure 1. Global annual average XCH_4 in 2021 derived from OPER-OFFL v 2.4.0 (a), OPER-RPRO v2.4.0 (b), and WFMD v2.0 (c). The spatial resolution is 7×7 km^2. The bad observations were masked using quality assurance values (qa_value ≥ 0.5 for operational data and qa = 0 for WFMD data).

support long-term analysis. Recent inversions in northern high latitudes (e.g. the North Slope of Alaska and Europe) showed that tundra emissions estimated from operational data align more closely with surface observation-based emissions, while WFMD-derived anthropogenic emissions over oil fields agreed more closely with in-situ measurements (Sicsik-Paré et al. 2025; Ward et al. 2025). As both retrievals exhibit a strong dependence on prior information and require rescaling of observation errors, intercomparisons between inversion frameworks and transport models are essential for TROPOMI inversions, particularly in high northern latitudes.

3. CH_4 emission quantification using TROPOMI data

To ensure a comprehensive survey, we collected peer-reviewed articles from the Web of Science Core Collection database. The search query was defined as *TS = ("methane" OR "XCH_4" OR "CH_4" OR "non-CO_2") AND TS = ("TROPOMI")*. The search period covered publications from 2018 to 2024, and the final search was performed on 1 March 2025. Two reviewers independently screened titles and abstracts to remove irrelevant studies, followed by full-text assessment against predefined inclusion criteria. Any discrepancies were resolved through discussion. Relevant information from each article—such as the study area, emission source, spatial scale, and quantification methods—was extracted. Finally, after excluding 21 articles related to general review, retrieval algorithm development, and validation of satellite products, a total of 133 articles focusing on the application of TROPOMI data for CH_4 monitoring were retained for analysis (see Supplementary Materials for details). No formal risk of bias or certainty assessment was conducted, as this review was descriptive and did not involve quantitative analysis.

CH_4 emissions originate from diverse sources, and the dominant sources vary significantly by location. The global CH_4 budget indicates that anthropogenic emitters (e.g. oil and gas facilities, coal mines, agriculture, and landfills) contribute up to 60% of total CH_4 emissions (Saunois et al. 2025). In contrast, natural sources, particularly wetlands, dominate emissions in tropical Africa and South America, driven by extensive wetland areas and high rates of organic decomposition. To account for this spatial and source-specific variability, the collected publications were categorized by spatial scale (global, regional, and local) and source type (anthropogenic and natural). This classification facilitates a more nuanced understanding of CH_4 dynamics and supports the formulation of targeted region- and sector-specific mitigation strategies.

Figure 2 shows the distribution of studies using TROPOMI CH_4 observations, categorized by spatial scale and source type. It should be noted that the numbers represent the frequency with which a specific sector or country was mentioned in the literature—many studies examined multiple sectors or countries within a single paper, so each sector or country was counted separately.

From the spatial perspective, 12 global-scale studies were identified, which mainly combined atmospheric chemistry transport models with atmospheric CH_4 and hydroxyl radical concentration to quantify global grid emissions (e.g. Qu et al. 2021; Yu et al. 2023). Second, 92 regional-scale studies were analyzed, of which 20% focused on the United States and 13% on China, followed by India, Africa, South America, and the Middle East (e.g. Kenea et al. 2021; Shen et al. 2022). The significant focus on the United States and China reflects their substantial contributions to global CH_4 emissions, as well as the availability of complementary datasets and policy-driven research initiatives (Crippa et al. 2025). Third, 29 studies focused on local-scale sources, using XCH_4 enhancements of large plumes to quantify emissions from facilities, such as landfills and oil/gas pipelines (e.g. Lauvaux et al. 2022; Wang et al. 2023).

From the perspective of source types, studies were categorized into anthropogenic sources (fossil fuels, waste, rice paddies, and livestock) and natural sources (wetlands). Studies focusing on fossil fuels, including coal, oil, and natural gas, accounted for nearly 40% of the total, indicating their critical role in global CH_4 emissions. Livestock emissions were the focus of 20% of the studies, while studies on waste, rice paddies, and wetlands were less frequent. Nevertheless, these results confirm the reliability of TROPOMI data in reducing the uncertainty associated with these sources.

3.1. CH_4 emission quantification at different scales

Global-scale studies mainly estimate the spatial and temporal patterns of CH_4 emissions across all source types on relatively coarse native grids of the inversion (~0.5°–2.5°, most commonly 2° × 2.5°), enabling

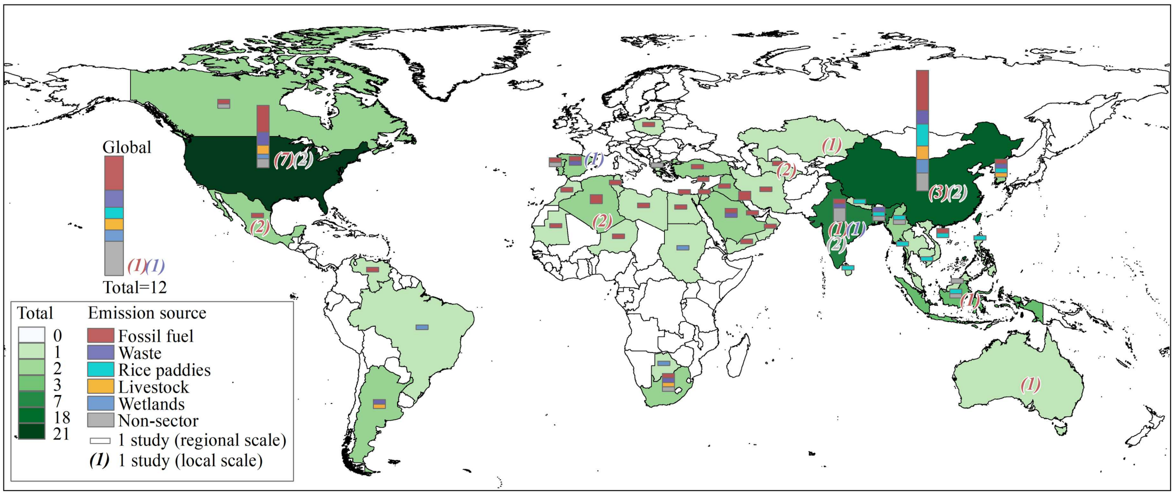

Figure 2. Distribution of studies utilizing TROPOMI data for CH_4 emission quantification of different emission sources at global, regional, and local scales. Note that some publications analyze multiple emission sources; in such cases, each source is counted separately in the source-type statistics. The total number of global-scale studies is labeled as "Total = 12", and the color bar labeled "Global" represents emission source counts, while the colored number in brackets represents two studies on global point sources. For each country, the total number of studies includes all publications conducted at both regional and local scales, and regional-scale studies are further categorized by emission source and represented by colored bars, while local-scale studies are indicated by colored numbers in brackets.

assessment of global CH_4 budget and sectoral attribution. Regional-scale analyses focus on basins, countries, or continents at higher resolution (commonly $0.25° \times 0.3125°$ or $0.5° \times 0.625°$), unveiling sources that were unresolved or underestimated in global inventories. Local-scale studies target point and city-scale sources, using TROPOMI data alone to quantify emissions from superemitters or in combination with high-resolution target satellites to detect and characterize individual plumes.

3.1.1. Global- and regional-scale CH_4 quantification

TROPOMI observations combined with inverse modeling have enabled the calculation of global sectoral CH_4 emission budgets at a spatial resolution of $2° \times 2.5°$ (Qu et al. 2021). Yu et al. (2023) further downscaled coarse-grid global inversions to produce $0.1° \times 0.1°$ gridded emission products by employing the GEOS–Chem adjoint model, a novel downscaling method, and independent constraints from observations of CH_4, CO, and OH. In addition, emissions from global fossil fuel exploitation are clearly resolved at 0.5° resolution using TROPOMI data, leading to substantial corrections to previous global inventories (Shen et al. 2023).

At the country scale, TROPOMI-based estimates provide independent constraints for national greenhouse gas inventories reported to the UNFCCC. For countries, such as China and Mexico, sectoral emissions have been quantified at fine spatial resolutions ($0.25° \times 0.3125°$) (Chen et al. 2022; Shen et al. 2021), with total emissions generally exceeding those inferred from GOSAT-based estimates. TROPOMI observations also enable a detailed characterization of the spatial distribution and seasonal variability of CH_4 emissions in individual oil and gas production basins (Shen et al. 2022; Zhang et al. 2020) and wetlands (Helfter et al. 2022).

In certain regions, TROPOMI data have revealed previously underestimated emissions using approaches that do not rely on a priori knowledge of sources, such as livestock emissions in the Permian Basin and fossil fuel emissions in parts of the Middle East (Liu et al. 2021, 2024; Roberts et al. 2023; Veefkind et al. 2023). However, retrieval biases and sparse valid observations in high-latitude and tropical regions remain major sources of uncertainty in CH_4 emission estimates (Lindqvist et al. 2024; Pandey et al. 2021; Tsuruta et al. 2023).

In addition to gridded emissions, some studies have estimated total emissions based on mean XCH_4 enhancements relative to surrounding background concentrations without explicitly resolving spatial emission distributions (Vanselow et al. 2024). Such approaches have been applied to quantify emissions from oil and gas production in the Permian Basin (Zhang et al. 2020), offshore and onshore regions in Mexico (Zavala-Araiza et al. 2021), and the seasonality of wetland emissions (Pandey et al. 2021).

3.1.2. City-scale CH_4 quantification

Approximately one-third of CH_4 emission plumes detected in TROPOMI data during 2021 are associated with city-scale sources (Schuit et al. 2023). City-scale CH_4 emissions differ from point sources and also require quantification methods different from global inversion approaches. In addition, cities are a key scale for climate policy implementation worldwide, but they often lack accurate inventory data, as they do not report to the UNFCCC. City-scale methane emissions are commonly quantified by combining atmospheric chemistry transport models (e.g. GEOS–Chem or WRF) with Bayesian inversion frameworks, or by applying observation-driven approaches, such as urban $\Delta CH_4/\Delta CO$ enhancement ratios, wind-assigned anomaly methods, and 2D Gaussian plume models to relate downwind concentration enhancements to city-wide emissions. Several studies have estimated emissions for individual cities in the United States, Canada, Mexico, South Asia, and South Korea (Hemati et al. 2024; Nesser et al. 2024; Plant et al. 2022; Suthar et al. 2024), attributing emissions primarily to natural gas, landfills, and untreated wastewater. These sources are commonly underestimated in bottom-up inventories of urban CH_4. Quantifying the relative contributions of these sources requires synergy with other types of observations, such as in-situ measurements (Tu et al. 2022a) and EM27/SUN observations (Park et al. 2024). Estimation accuracy can also be improved through advanced XCH_4 retrieval algorithms (de Foy et al. 2023) and the use of tracer gases [e.g. NO_2 (Tu et al. 2022a) and CO (Plant et al. 2022)].

3.1.3. Point-source scale CH_4 quantification

TROPOMI data alone can detect individual point sources with emission rates exceeding 1000 kg h^{-1}, while synergy with target satellites enables the detection of emission plumes (Duren et al. 2019; Jacob et al. 2022). Anthropogenic CH_4 sectors, such as oil and gas fields (Cusworth et al. 2018; Maasakkers et al. 2022a), landfills (Cusworth et al. 2020; Maasakkers et al. 2022b; Tu et al. 2022b), and coal mines (Sadavarte et al. 2021), are often associated with large-scale and episodic emission events. Methods for quantifying point-source emissions include Gaussian plume inversion, mass-balance approaches, Lagrangian particle models, wind-assigned anomaly analysis, cross-sectional flux calculations, and the integrated mass enhancement (IME) method (Table 2).

First, Gaussian plume inversion estimates emissions by fitting a two-dimensional Gaussian model to observed plume enhancements. For instance, CH_4 emissions from wastewater sources in 61 global cities have been mapped using this approach (de Foy et al. 2023). However, the Gaussian plume model encounters limitations under inhomogeneous wind conditions, for distant observations, or when plumes are small and transient (He et al. 2024; Krings et al. 2011).

Second, the mass balance method estimates the CH_4 emission rate by integrating the measured CH_4 enhancements with the wind speed (Jacob et al. 2016). This approach has been applied to quantify emissions from oil and gas fields and natural gas blowouts (Mazzini et al. 2021; Pandey et al. 2019), demonstrating TROPOMI's capability to detect major leakage events. However, the traditional mass balance method cannot properly parameterize turbulence in small-scale, transient plumes (Varon et al. 2018). To address this, an improved mass balance approach was developed and applied to facility-level emissions in Mexico (Zavala-Araiza et al. 2021). Regarding wind information, ERA5 and WRF-based meteorological fields provide accurate site-specific estimates (Pandey et al. 2021; Pandey et al. 2019). The associated uncertainty can also be qualified using Buchwitz's empirical equation (Zhang et al. 2020).

Third, Lagrangian particle models (e.g. STILT and HYSPLIT) combined with automatic plume detection algorithms can mitigate the impact of plume overlap caused by variable winds (Lauvaux et al. 2022). These methods improve the accuracy of emission estimates by accounting for downwind emission dispersion and reducing sensitivity to local background concentrations (Varon et al. 2018). Two optimized methods—wind-assigned anomaly and cross-sectional flux—have been applied to local-scale CH_4 emission quantification (Pandey et al. 2019; Sadavarte et al. 2021; Tu et al. 2022b). For example, Tu et al. (2022a) estimated landfill emissions in the Madrid metropolitan area using the wind-assigned anomaly techniques by isolating the

Table 2. Methods of regional CH_4 emission quantification using TROPOMI.

Scale	Reference	Method	XCH_4 data product	Dominant application	Limitations
Global	• Global sectors (Qu et al. 2021); global oil-gas and coal mine (Shen et al. 2023) • Global sectors (Yu et al. 2023) • Global persistently enhanced CH_4 (Vanselow et al. 2024)	• GEOS–Chem + analytical Bayesian inversion • GEOS–Chem adjoint model + 4D-var inversions • Persistent hotspot detection (PHD) algorithm	• OPER-OFFL; OPER-OFFL • OPER-RPRO • WFMD v1.8	• Assessing CH_4 budget • Trend analysis	• Sectoral attribution relies on the accuracy of prior information
Regional	• Sectors across Venezuela (Nathan et al. 2024) • Sectors across China (Chen et al. 2022); oil and natural gas production basins in the USA and Canada (Shen et al. 2022); Permian Basin, USA (Zhang et al. 2020) • Permian Basin, USA (Varon et al. 2023) • Okavango Delta, Botswana (Helfter et al. 2022); Oil and gas, Uganda (Humpage et al. 2024) • Sudd, South Sudan (Pandey et al. 2021); oil and gas production in offshore/onshore Mexico (Zavala-Araiza et al. 2021); • Permian basin, USA (Veefkind et al. 2023); Permian basin, USA (Roberts et al. 2023); Permian basin, USA (Liu et al. 2021a); Middle East (Liu et al. 2024)	• Weather Research and Forecasting (WRF)–Chem + analytical Bayesian inversion • GEOS–Chem + analytical Bayesian inversion • GEOS–Chem model + Kalman filter inversion • GEOS–Chem + Ensemble Kalman Filter (EnKF) inversions • Mass balance • Divergence method	• OPER-OFFL • OPER-RPRO; OPER-RPRO; OPER-OFFL • OPER-RPRO • OPER-RPRO; OPER-OFFL • OPER-OFFL;—WFMD; OPER-OFFL; OPER-OFFL; WFMD	• Constraints of the country UNFCCC reports • Middle-latitude monthly and annual estimates • Previous unknown sources • Seasonal variations in wetland CH_4 emissions	• Large systematic errors over high-latitude and tropical regions ; • Heterogeneity of sources
City-scale	• 6 cities in Canada, the USA, and Mexico (Hemati et al. 2024) • 95 US cities (Nesser et al. 2024) • 8 US cities (Plant et al. 2022) • Madrid, Spanish (Tu et al. 2022a) • 4 cities in South Asia (Maasakkers et al. 2022b) • Waste water in global 61 cities (de Foy et al. 2023) • 5 Indian cities (Suthar et al. 2024); Seoul, South Korea (Park et al. 2024)	• GEOS–Chem + 3D inversion • GEOS–Chem + analytical Bayesian inversion • Urban $\Delta CH_4/\Delta CO$ enhancement ratio • Wind-assigned anomaly method • Weather Research and Forecasting (WRF) model + analytical Bayesian inversion • 2D Gaussian model	• OPER-OFFL • OPER-RPRO • OPER-OFFL • OPER-RPRO • OPER-RPRO • OPER-RPRO • OFFL/L3_CH_4	• The first area-flux imager for city-scale emission estimates • Synergy with tracer gas	• Source attribution is limited by pixel mixing of multiple sources and background
Point-source	See Table 3	See Table 3	See Table 3	• Estimation of known and unknown supersource emission • Locating for the target satellite	• Retrieval of plumes is sensitive to wind • Not facility-level estimates

Note: The studies listed for each method are examples. A comprehensive list of all studies corresponding to each approach and TROPOMI XCH_4 product is provided in the Supplementary Material.

Table 3. Methods for local-scale CH_4 emission quantification using TROPOMI.

Method	Reference	Advantages	Limitations
2D Gaussian model	Waste water in global 61 cities (de Foy et al. 2023)	• Fast fit and localization of a single strong plume near the sources	• Overlapping plumes or strongly varying winds
Mass balance	(1) Oil and gas field in Indonesia (Mazzini et al. 2021); (2) Livestock production, agriculture, and biomass-burning sectors in Argentina (Puliafito et al. 2020); (3) Oil and gas production in offshore/onshore Mexico (Zavala-Araiza et al. 2021)	• Total emission estimates from a strong, relatively isolated plume across a transect	• Highly sensitive to wind and background • Weak and multiple sources
Lagrangian particle dispersion model	(1) Oil and gas basins across the world (Lauvaux et al. 2022); (2) Basins of the United States (Cusworth et al. 2022)	• Inversing nonuniform and instantaneous emissions of point and area sources • Complex wind and transport with long downwind distances	• Requirement of fine meteorology data and high computational cost
Wind-assigned anomaly method	(1) Landfill in Madrid, Spain (Tu et al. 2022b); (2) Coal mine in Shanxi, China (Tu et al. 2024)	• Only XCH_4 and wind data • Rapid screening of dominant upwind source directions for many cities	• Weak or mixed sources
Cross-sectional flux methods	(1) Coal mines in Australia (Sadavarte et al. 2021); (2) Single plume (Pandey et al. 2023)	• Plumes intersected by the track • Strong sources	• Dependence on steady plume and wind; • Sensitive to cross-section placement and background settings • Weak or partially sampled plumes
Bayesian optimal estimation method	Permian basin, USA (Cusworth et al. 2021b)	• Explicit uncertainty estimates	• Sensitive to prior and error-covariance assumptions • Weak or unknown sources can be missed
Integrated Mass Enhancement (IME) method	(1) Global 2974 plumes in 2021 (Schuit et al. 2023); (2) A well blowout in Kazakhstan (Guanter et al. 2024)	• Isolated • Strong point sources at a single overpass	• Weak and multiple sources
Mass balance and cross-sectional flux methods	A well blowout in Ohio, USA (Pandey et al. 2019)	• Isolated or a few plumes by cross-validation of two independent approaches	• Weak and multiple sources

signal near emission source from the CH_4 background, while Sadavarte et al. (2021) estimated emissions from three Australian coal mines using the cross-sectional flux method.

Finally, the IME method links total plume mass to source rates and incorporates turbulent diffusion effects via effective wind speed (Guanter et al. 2024; Pandey et al. 2023; Schuit et al. 2023). Machine learning methods based on convolutional neural networks can infer source rates without explicit wind speed information (Jongaramrungruang et al. 2022), offering promising potential, though they have yet to be fully integrated with TROPOMI observations.

Using limited snapshot measurements for the quantification of time-averaged CH_4 emissions from intermittent point sources can lead to substantial biases. However, some highly intermittent emissions by design may have predictable diurnal or longer-term variations, such as short-term intermittency in oil and gas infrastructure (liquids unloading, blowdowns, and startups) (Cusworth et al. 2021a; Duren et al., 2019) and long-term variability related to operating practices and the facility life cycle (Varon et al. 2021). It is essential to explicitly account for either emission frequency or persistence and use observations with repeated return times and at different times of day (Cusworth et al. 2021a; Schissel and Allen 2022). Existing TROPOMI data are mainly applied to emission estimates of single events from point sources (instantaneous or persistent), and the increased frequency of observation can identify the persistence of emissions to enable corrective action (Cusworth et al. 2022; Lauvaux et al. 2022).

3.2. CH_4 sectoral attribution

TROPOMI enables sectoral attribution from top-down total emission estimates when combined with prior inventories or tracer gases. For fossil fuel and waste sources, TROPOMI-based emission estimates at global and regional scales are comparable to other satellite-based assessments, and facility-level emissions can be further constrained by synergistic use with high-resolution target sensors. By contrast, livestock emissions are spatially diffuse, typically colocated with other rural sources, and often lack specific coemitted tracers, making them difficult to isolate from regional background variability. Wetland and rice paddy emissions are generally large-area sources with significant seasonal variations. However, the retrieval performance and source attribution for these sources are often limited by mixed pixels, persistent cloud cover, low surface albedo, and model representation errors, especially in tropical regions. Overall, the dense, near-global coverage and relatively high spatial resolution of TROPOMI observations have revealed many previously unknown strong point sources and natural emitters, whereas diffuse agricultural emissions remain more challenging and require integration with accurate bottom-up estimates.

3.2.1. Fossil fuel

Fossil fuel exploitation (oil, gas, and coal) CH_4 emissions account for about 40% of global anthropogenic CH_4 emissions, with the U.S., Russia, Venezuela, and Turkmenistan being the largest emitters. These emissions typically occur either as sustained, highly aggregated releases from production basins or as episodic, large CH_4 releases caused by sudden leakage events. TROPOMI data enable reliable quantification of emissions from high-emitting basins (>0.5 Tg a^{-1}), and its dense midlatitude coverage allows for constraints with posterior uncertainties less than 30% (2σ) (de Gouw et al. 2020; Shen et al. 2022). Global CH_4 emissions from fossil fuels were successfully derived from improved TROPOMI products via inversion analysis at resolutions up to 0.45°, revealing underestimation in national bottom-up inventories (Shen et al. 2023). These results largely update the previous estimates by Qu et al. (2021), which were affected by artifacts in early TROPOMI data versions.

The United States has been a hotspot for studying fossil fuels-related CH_4 emissions, particularly in the Permian Basin, which is the largest oil- and second-largest natural gas-producing region in the country. Inversion analyses using GEOS–Chem and inventories, such as GFEI v25 or EDGAR estimated regional emissions at ~2.8 Tg a^{-1} (Shen et al. 2022; Zhang et al. 2020), while CH_4 plume detection highlighted CH_4 leakage issues from oil and gas facilities (Cusworth et al. 2021b). This modeling framework has since been extended globally to regions, including Mexico, Canada, China, the Middle East, and North Africa, significantly refining fossil fuel CH_4 emission inventories (Shen et al. 2021). For example, UNFCCC-reported emissions require upward corrections of 103% for natural gas in the Middle East and downward corrections of 14% for oil in North Africa (Chen et al. 2023). In China, reported emissions require upward adjustments of 147% for oil and upward of 61% for natural gas, but a downward adjustment of 15% for coal due to uncertainties in emission factors and leakage rates (Chen et al. 2022). Coal mining emissions in China are more specifically from Shanxi Province, where annual emissions were estimated at approximately 8–9 Tg a^{-1}, which is close to bottom-up estimates (Peng et al. 2023). However, local-scale estimates of annual emissions showed the inconsistency with bottom-up inventories and could be related to the lack of observations of extreme emission events during TROPOMI overpasses in this region (Bai et al. 2024; Tu et al. 2024). Additionally, an improved divergence method has also been developed to estimate CH_4 emissions for the Permian Basin and the Middle East, yielding results consistent with chemical transport model (CTM)-based inversions (Liu et al. 2021, 2024; Veefkind et al. 2023).

Superemitters related to the fossil fuel industry can also be detected using TROPOMI data. These events are mainly caused by leakages during operations or equipment failures and are often overlooked in inventories. Global oil and gas ultraemitters (>25 t h^{-1}) have been systematically detected by Lauvaux et al. (2022). Notable examples include a gas well explosion in Ohio that emitted the equivalent of one quarter of the state's annual oil and gas CH_4 emissions (Pandey et al. 2019), six coal mines in Queensland that together contributed 55% of Australia's coal mine emissions (Sadavarte et al. 2021), and a blowout in Louisiana that exceeded all previously known US point-source emissions at the time (Maasakkers et al. 2022a). Consequently, these findings demonstrate that remote-sensing instruments are critical for detecting such high-impact events and enabling timely mitigation through monitoring, regulation, and infrastructure improvement (Zhang et al. 2020).

3.2.2. Waste

Nearly 70% of waste is currently disposed of in landfills or open dumping sites (Dogniaux et al. 2025). Many of the landfill-related sources were initially identified at a coarse resolution with TROPOMI and were subsequently pinpointed to their exact locations through follow-up observations from high-resolution target satellites. For example, XCH_4 anomalies were detected at a large-scale landfill in the northwestern part of Jinan city in China (Zhang et al. 2022) and at the Sunshine Canyon landfill in the Los Angeles Basin in the USA (Cusworth et al. 2020). Global waste-related CH_4 emissions derived from TROPOMI observations are estimated at 83 (79–87) Tg a^{-1} (Yu et al. 2023), with landfill CH_4 emissions accounting for about 44 Tg a^{-1} (Qu et al. 2021). This sector has consequently become a major study hotspot. Landfill emission rates were derived in Argentina, Pakistan, India, and Spain using the local-scale quantification methods (Maasakkers et al. 2022b; Tu et al. 2022c), which corrected the underestimation of the UNFCCC report. Additionally, wastewater represents another waste source, primarily in city-scale sources. Wastewater CH_4 emissions in 61 cities worldwide have been found to increase substantially with increasing volumes of untreated wastewater (de Foy et al. 2023; Zhang et al. 2021).

3.2.3. Livestock

Livestock CH_4 emissions originate from the manure and enteric fermentation of ruminants, such as dairy and beef cattle, while there is a wide range of existing estimates (Blaustein-Rejto and Gambino 2023). Satellite observations help to pinpoint the source of CH_4 plumes across scales, from individual farms to broad regions. TROPOMI-based estimates of global livestock CH_4 emissions have been relatively stable in recent years, reaching 139 Tg a^{-1} in 2021 (Qu et al. 2021) and 132 (127–136) Tg a^{-1} in 2023 (Yu et al. 2023). In China, livestock accounts for ~19% of national emissions (Li et al. 2023), representing an upward correction of 37% relative to the UNFCCC report, especially in northern provinces. In India, which holds over 35% of the world's cattle and 20% of buffaloes, the upward revision in recent CH_4 estimates relative to earlier studies is primarily attributed to increasing livestock emissions (Qu et al. 2021). In addition, livestock CH_4 emissions have been detected for the first time in the Central Valley of California (Schneising et al. 2019), quantified for the first time in the northern Permian Basin of the United States (Liu et al. 2021a), and revealed the underestimation in Brazil due to the transition of local forests to agricultural land (Nepstad et al. 2019; Yu et al. 2023; Zhang et al. 2021).

3.2.4. Rice paddies

Rice paddies typically exhibit a relatively low emission rate per unit area, which frequently results in undetectable plumes. Additionally, substantial fluctuations in overall emissions occur following extensive changes in rice fields and alterations in fertilizer and water management, thereby requiring prompt and continuous monitoring (Chen et al. 2025). Rice sources are concentrated in Asian monsoon countries, where TROPOMI XCH_4 exhibits seasonal variations strongly correlated with the rice growth cycle (Hari et al. 2022; Kozicka et al. 2023; Kozicka, Gozdowski, and Wojcik-Gront 2021). TROPOMI-derived estimates often lead to upward corrections of emission inventories, particularly in China. Qu et al. (2021) used GEOS–Chem and found higher emissions than those in EDGAR, although the coarse spatial resolution ($2° \times 2.5°$) and source misclassification (rice vs. coal) led to inconsistencies with GOSAT results (Sheng et al. 2019). Chen et al. (2022) effectively separated coal and rice emissions using an improved coal emission inventory at a finer scale (25 km) and optimized the allocation of emissions via a Gaussian mixture model (Chen et al. 2022). Their findings suggested an upward correction for rice (+34%) and a downward correction for coal (−15%). Liang et al. (2024) further derived annual and monthly rice CH_4 emissions in China's Heilongjiang Province using the GEOS–Chem model. In South Asia and Southeast Asia, total CH_4 emissions were also higher than emission inventories, with a 45% upward correction required for the rice growing period from July to October (Yu et al. 2023). Generally, TROPOMI observations capture spatiotemporal variations of CH_4 concentration in rice-growing regions, facilitating more accurate national reports.

3.2.5. Wetlands

Wetland CH_4 emissions are usually intermittent and dynamic; consequently, their estimates remain subject to large uncertainties (Lin et al. 2024). TROPOMI-based studies on natural wetland CH_4 emissions are currently limited but have confirmed promising performance due to dense spatial–temporal observations. Hu et al. (2018) identified CH_4 enhancement over the Sudd wetlands in South Sudan using only 1 month of data, a result consistent with 7-year SCIAMACHY averages (Hu et al. 2018). Li et al. (2024b) found that dry-season TROPOMI XCH_4 in the Pantanal region of South America was two to three times higher than bottom-up predictions. In China, TROPOMI-derived wetland CH_4 estimates corrected the UNFCCC inventory upward by 1.1 Tg a^{-1} (Chen et al. 2022). However, spatial overlap with livestock and rice sources often obscures the contribution of natural wetland sources. Regionally, Liu et al. (2021a) applied an improved divergence method to derive wetland CH_4 emissions in the eastern Permian Basin, finding results consistent with WetCHARTs spatial patterns (Liu et al. 2021a). Notably, although tropical and high-latitude (e.g. Russia and Canada) wetlands are major CH_4 sources, few studies quantified wetland emissions from these areas using TROPOMI data so far. For example, the emissions from the Oka Delta and Sudd in Africa were estimated using GEOS-Chem CTM models and the mass balance method, respectively (Helfter et al. 2022; Pandey et al. 2021). Tsuruta et al. (2023) used TROPOMI data and the CTE-CH_4 atmospheric inverse model to provide the first monthly estimates of northern high-latitude wetland CH_4 emissions (Tsuruta et al. 2023). The estimated magnitude and seasonality were consistent with ground-based measurements and wetland extent maps, highlighting biases in current bottom-up models.

Wetland CH_4 emissions estimation is strongly impacted by environmental factors, such as soil temperature and surface water extent. Previous efforts (Yu et al. 2023) pointed out that WetCHARTs, a prior inventory of wetland sources for CTMs, uses surface temperature rather than soil temperature, leading to an underestimation of posterior emissions. Surface water area expansion driven by rainfall shows a strong correlation with wetland CH_4 emissions in tropical and subtropical regions ($R > 0.7$) (Jensen and McDonald 2019). However, TROPOMI observations during the rainy season were often scarce due to thick cloud cover (Qu et al. 2021). Furthermore, bias in retrieval algorithms due to the low albedo of wetlands and spatial overlap between wetlands and agriculture indicates that more attention is needed to accurately derive wetland CH_4 emissions using the TROPOMI observations (Karoff and Vara-Vela 2023).

4. Discussion

4.1. TROPOMI's role in the satellite-based CH_4 monitoring system

Given that atmospheric CH_4 has a high warming potential, timely, scalable, and independent atmospheric monitoring is essential for tracking and constraining human activities in support of climate action (IPCC 2023). Furthermore, it is crucial for improving the understanding of land–atmosphere feedbacks to enable more accurate modeling of natural sources (Lin et al. 2024; Zhang et al. 2023). TROPOMI provides global measurements with dense spatial and temporal coverage. Our review of existing applications shows that TROPOMI retrieval algorithms have been widely established and validated, achieving state-of-the-art capabilities in high-precision spatiotemporal monitoring at finer scales and in identifying previously unknown local sources globally. However, several limitations of this review should be noted. Relevant research from other databases may have been omitted because of availability. Additionally, no formal assessment of risk of bias or meta-analysis was conducted, limiting the quantitative synthesis of findings.

To clarify TROPOMI's unique role in the satellite-based CH_4 monitoring system, we compared its applications with two pioneering missions, GOSAT and GHGSat (Table 4).

TROPOMI and GOSAT/GOSAT-2 are both area-flux imagers designed to estimate CH_4 emissions by sector and country and to support global stocktakes (Worden et al. 2022; Yu et al. 2023). Independent global studies have concluded that, although both satellites derive comparable emission estimates with similar retrieval precision at large scales, discrepancies emerge at finer spatial scales due to their different spatiotemporal sampling and retrieval biases (Liang et al. 2023; Liu et al. 2021a; Qu et al. 2021). TROPOMI's dense coverage and relatively high spatial resolution can identify more localized CH_4 enhancements that were previously unresolved by GOSAT, and its daily revisit frequency allows for the tracking of rapidly evolving sources on a weekly timescale (Varon et al. 2023), such as oil and gas blowouts, coal mine accidents, wetland flooding, and rice paddy growth (Chen et al. 2022; Liang et al. 2024; Pandey et al. 2021). In contrast, long-term GOSAT/GOSAT-2 XCH_4 records are more commonly applied to large-scale (continental or national) trend analysis, background concentration estimation, and supplementary constraints for other satellite products (e.g. TROPOMI) (Baray et al. 2021; Hancock et al. 2025; Maasakkers et al. 2022a; Parker et al. 2020; Zhong et al. 2025).

The target satellites, taking GHGSat as an example, are designed to pinpoint CH_4 point-source emissions at the facility scale (Jervis et al. 2021). GHGSat is a constellation of 11 CH_4-focused satellites (and one CO_2-focused satellite), imaging scenes of approximately 12×15 km^2 at very high spatial resolution (25×25 m^2)

Table 4. Comparisons of the capabilities of TROPOMI with the GOSAT and GHGSat instruments.

	TROPOMI	GOSAT/GOSAT-2	GHGSat
Spatial resolution	5.5×7 km^2	10.5/9.7 km (diameter, circular)	25×25 m^2
Revisit time	1 day	3/6 days	14 days (per satellite)
Absorption band for CH_4 (nm)	2305–2385	1626–1695	1630–1675
Coverage	Global, continuous swath	Global, discrete points	Targeted sites
Swath	2600 km (push-broom imaging)	Discrete, 1–9/5 points in ~1000 km	12×12 km scene (pointing mode)
Precision	0.70%–0.72%[a]	0.70%–0.8%[a]	2%–5%[b]
Bias	−0.36% to +0.20%[a]	−0.05 to 0.22%[a]	Scene-dependent[b]
Scale	Regional to global; ultra sources at local scale	Regional to global	Facility or equipment level at local scale
Source detection	Oil & gas fields, coal mines, landfills, wetlands, agriculture (e.g. rice paddies)	Oil & gas fields, coal mines, landfills, wetlands, agriculture (e.g. rice paddies)	Oil & gas facilities, coal mine ventilation shafts, individual landfills, power plants
Domain application	Large-scale emission patterns; detecting ultra-transient events	Long-term trends; cross-calibration with other satellites and ground-based networks	Targeted pinpoint; regulatory compliance

[a] TROPOMI, GOSAT, and GOSAT-2 precision and biases would be different for each product, but even for different versions of each product, we give a range of biases of satellite-TCCON of the latest version. TROPOMI: WFMDv2.0 (Schneising et al. 2025), OPERv02.08.00 (standard and bias-corrected) (Lambert et al. 2025); GOSAT: v2.3.8; and GOSAT-2: v2.1.0 (proxy and full physics) (Barr et al. 2025).
[b] On average for the C1/C2–C5 satellites of the constellation (McLinden et al. 2024).

(McLinden et al. 2024). Such instruments enable plume detection at the facility or equipment level (e.g. individual oil wells, small landfills, and pipeline valves) with high sensitivity (>100 kg h^{-1}) (Jervis et al. 2025; McLinden et al. 2024). In contrast, TROPOMI—despite being an area-flux imager—has shown the ability to detect previously unknown ultraemitters with global near-daily coverage (e.g. large-scale oil fields, landfills, and pipeline leaks) (Table 3). However, its spatial resolution is coarser than the facility level, and its detection threshold is limited (>1000 kg h^{-1}) (Jacob et al. 2022). In cases where both instruments observe the same event, TROPOMI and GHGSat generally show consistent plume patterns, but TROPOMI has a more limited ability to separate closely spaced plumes due to its coarser spatial resolution (Schuit et al. 2023). Conversely, TROPOMI's emission estimates for the same period were often higher by capturing broader plume extents and continuous emissions over time, while the early GHGSat satellite missed parts of the plume extent and peaks due to its narrower swath and limited temporal coverage (Lauvaux et al. 2022). With the current GHGSat constellation, combined coverage can now detect more than ten thousand plumes worldwide (Jervis et al. 2025).

4.2. Challenges and perspectives

CH_4 emission monitoring based on TROPOMI data still faces challenges, pertaining to the quality of TROPOMI data product, the availability of validation data, and the accuracy of CH_4 emission estimates. Future research perspectives are proposed to address existing limitations and optimize the performance of future missions.

4.2.1. TROPOMI retrieval correction and validation

Systematic errors in current operational TROPOMI XCH_4 retrievals can be mitigated through improved representation of surface optical properties and aerosol vertical profiles (Lorente et al. 2023). The forward-model characterization could be improved by incorporating scene-dependent forward-model error covariance matrices (binned by surface albedo, viewing geometry, and land-cover type) into the optimal-estimation framework. In addition, aerosol prior information should be further strengthened from other satellite observations (Somkuti et al. 2025). Furthermore, the strict empirical threshold-based quality filtering of operational data could be replaced by more refined approaches based on machine learning, updated training datasets, and a new VIIRS cloud product (Barr et al. 2025; Schneising et al. 2023, 2025).

The uncertainty of TROPOMI retrievals can further be mitigated through synergy with other datasets, such as ground-based observations and other XCH_4 satellite products. There is a critical need to expand current networks in wetlands and rice paddies, which would offer enhanced spatial–temporal cross-validation and reduce systematic biases (Helfter et al. 2022; Humpage et al. 2024; Park et al. 2024). In addition, GOSAT instrument is characterized by high spectral resolution and can be combined with high-density TROPOMI data via machine learning. Such a combination has been shown to effectively correct biases and artifacts in TROPOMI XCH_4 OPER data (Balasus et al. 2023). For example, Chen et al. (2022) optimized TROPOMI OPER data reliability by removing outliers that deviated by >20 ppb from GOSAT. GOSAT-2 XCH_4 products retrieved with RemoTeC and a novel random forest classifier for quality filtering span from 2019 to 2023 and show close agreement with TROPOMI (OPER v2.4.0), with high correlations exceeding 0.85; this ensures robust results by combining these two datasets (Barr et al. 2025). The upcoming GOSAT-GW mission will carry the Thermal and Near-infrared Sensor for Carbon Observation-3 (TANSO-3), operating by default in push-broom mode with a footprint size of 10 km and a swath of 911 km (Tanimoto et al. 2025). The integration of Infrared Atmospheric Sounding Interferometer (IASI) profiles and TROPOMI XCH_4 data better constrains upper tropospheric/stratospheric CH_4 variations and further enables the detection of CH_4 variations near the surface (Schneider et al. 2022; Shahzadi et al. 2025). In the future, multisatellite fusion data, such as the global CH_4 product generated from SCIAMACHY and GOSAT for 2003–2018, may be instrumental in validating TROPOMI XCH_4 long-term records (Reuter et al. 2020). The latest Sentinel-5 UV-VIS-NIR-SWIR spectrometer (UVNS) onboard the MetOp-SG-A1 satellite includes a SWIR band at 1595–1675 nm and enables SWIR-based proxy-CO_2 XCH_4 retrievals that are less sensitive to cloud, surface albedo, and reflectance effects, thereby providing improved spatial coverage. Such proxy-based products are expected to complement TROPOMI full-physics retrievals in future multimission CH_4 analysis (ESA 2025).

4.2.2. Improvement of CH_4 emission estimate

Accurate satellite-based prior information regarding natural and anthropogenic emission sources is essential for improving CH_4 emission estimates. On the one hand, characterizing the spatial distribution (e.g. wetlands and rice paddies) based on high-resolution multispectral instruments (e.g. Sentinel-2 and Landsat) enables the refinement of the prior emission inventories by enhancing the representation of bottom-up models or data-driven methods (Chen et al. 2025). On the other hand, coemitted tracers can provide a better prior reference for sectoral attribution, such as TROPOMI data-derived NO_2 for oil and gas production (Roberts et al. 2022), CO for anthropogenic sources (Yu et al. 2023), and NH_3 for livestock (Tang et al. 2025). In addition, joining multisatellite independent observations improves the posterior XCH_4 for inverse modeling. For instance, the combination of GOSAT and TROPOMI-derived global nonwetland CH_4 emissions yielded a degrees of freedom for signal (DOFS) of 244 for the annual inversion, significantly outperforming the DOFS of 151 achieved by TROPOMI alone (Qu et al. 2021). TROPOMI data integrated with target-mode observations can effectively pinpoint source locations and provide robust CH_4 enhancement detections. For example, TROPOMI combined with VIIRS thermal data captured CH_4 emissions during the flaring and venting phases of a well blowout (Maasakkers et al. 2022a); similarly, GHGSat instruments targeted locations with strong TROPOMI XCH_4 enhancement and quantified facility-level landfill emissions in India, Argentina, and Pakistan (Maasakkers et al. 2022b). A TROPOMI–PRISMA two-tier framework revealed facility-scale sources ($30 \times 30\ m^2$) in China, the USA, and Iraq (Wang et al. 2023). IASI and TROPOMI data directly derived tropospheric XCH_4 enhancement related to source emissions from the surface to 7 km as well as background variations related to stratospheric XCH_4 (Tu et al. 2022a). It is also possible to identify strong CH_4 sources (e.g. leakage) with unprecedented precision through synergy with other high-resolution data, such as the current EnMAP, Carbon Mapper, Gaofen5 series (Li et al. 2024a), Sentinel-2/3 (Pandey et al. 2023), and upcoming missions like CHIME and CO2M satellites (Mohammadimanesh et al. 2025).

Chemical Transport Model (CTM)-based CH_4 inversions (e.g. GEOS-Chem, WRF, TM5) are strongly dependent on prior inventories and are experiencing a computational bottleneck due to the increasing spatiotemporal resolution of dense atmospheric observations. Machine learning approaches offer automatic differentiation or data-driven source–receptor relationships without the need for computationally expensive explicit Jacobian matrix construction, thereby enabling rapid, high-resolution, large-scale, and multiyear CH_4 emission inversions (Dadheech, He, and Turner 2025). In addition, the Integrated Methane Inversion (IMI 1.0) cloud platform, hosted on Amazon Web Services, allows direct access to the Bayesian optimal grid for emission estimation (Varon et al. 2022). It enables quality control of TROPOMI data and inversion outputs, facilitates flexible prior inventory modification, and generates emission ensembles and error statistics with reduced time cost once the Jacobian matrix is constructed. IMI v1.0 has been applied to estimate annual emissions in the Permian Basin (3.9 Tg a^{-1})—a 45% increase over the inversion results of Zhang (Zhang et al. 2020)—with a DOFS of 10.8 (Varon et al. 2022). In Denmark, IMI v1.0 revealed that prior estimates underestimated national emissions by 66% (Vara-Vela et al. 2024). IMI v2.0 was released and has substantial development in spatiotemporal resolution, point source monitoring, and so on (Estrada et al. 2025). An annual inversion with 28-day temporal resolution at 25×25 km^2 resolution for the contiguous US was derived, which is in agreement with the range of emission estimates reported in other studies.

5. Conclusions

New satellite observations with enhanced spatiotemporal coverage will strengthen the global CH_4 monitoring system, bridging scales from global to local and supporting climate action. The TROPOMI instrument provides powerful capabilities for continuous CH_4 monitoring; however, fully exploiting its potential requires a comprehensive understanding of its performance and limitations.

In this work, we reviewed current TROPOMI applications across multiple spatial scales, from global to local, and across various source types, from natural to anthropogenic. TROPOMI data, when combined with chemical transport models or the mass balance approach, enable the fine-scale quantification of area-source emissions. Furthermore, when integrated with target satellites and plume models, it facilitates the detection of point-source emissions. Future progress in broadening applicability and improving efficiency can be achieved by optimizing the retrieval algorithm, expanding ground-based observation networks, advancing joint multisatellite monitoring, and refining prior inventories. Additionally, leveraging machine learning approaches for inverse modeling will be crucial.

Author contributions

CRediT: **Ruoqi Liu:** Data curation, Formal analysis, Writing – original draft; **Siqi Li:** Data curation, Writing – original draft; **Geli Zhang:** Conceptualization, Funding acquisition, Supervision, Writing – review & editing; **Mengyao Liu:** Writing – review & editing; **Xiao Lu:** Writing – review & editing; **Shushi Peng:** Writing – review & editing; **Lu Shen:** Writing – review & editing; **Yuzhong Zhang:** Writing – review & editing; **Minghao Zhuang:** Writing – review & editing; **Xiaoxing Zuo:** Writing – review & editing; **Jinwei Dong:** Writing – review & editing.

Disclosure statement

No potential conflict of interest was reported by the author(s).

Funding

This work was supported by the National Natural Science Foundation of China (42171115).

ORCID

Ruoqi Liu 0000-0003-1704-1151

Data availability statement

The data that support the findings of this study are available in Figshare https://doi.org/10.6084/m9.figshare.29908439.v2.

Registration and protocol

This review was not registered in any database. No formal review protocol was prepared prior to conducting the review. No amendments were made to the planned methodology during the review process.

References

Alberti, C., Q. Tu, F. Hase, M. V. Makarova, K. Gribanov, S. C. Foka, V. Zakharov, et al. 2022. "Investigation of Spaceborne Trace Gas Products over St Petersburg and Yekaterinburg, Russia, By Using Collaborative Column Carbon Observing

Network (COCCON) Observations." *Atmospheric Measurement Techniques* 15: 2199–2229. https://doi.org/10.5194/amt-15-2199-2022.

Bai, S., Y. Zhang, F. Li, Y. Yan, H. Chen, S. Feng, F. Jiang, et al. 2024. "High-Resolution Satellite Estimates of Coal Mine Methane Emissions from Local to Regional Scales in Shanxi, China." *Science of the Total Environment* 950: 175446. https://doi.org/10.1016/j.scitotenv.2024.175446.

Balasus, N., D. J. Jacob, A. Lorente, J. D. Maasakkers, R. J. Parker, H. Boesch, Z. Chen, M. M. Kelp, H. Nesser, and D. J. Varon. 2023. "A Blended TROPOMI + GOSAT Satellite Data Product for Atmospheric Methane Using Machine Learning to Correct Retrieval Biases." *Atmospheric Measurement Techniques* 16: 3787–3807. https://doi.org/10.5194/amt-16-3787-2023.

Baray, S., D. J. Jacob, J. D. Maasakkers, J. X. Sheng, M. P. Sulprizio, D. B. A. Jones, A. A. Bloom, and R. McLaren. 2021. "Estimating 2010–2015 Anthropogenic and Natural Methane Emissions in Canada Using ECCC Surface and GOSAT Satellite Observations." *Atmospheric Chemistry and Physics* 21: 18101–18121. https://doi.org/10.5194/acp-21-18101-2021.

Barr, A. G., J. Landgraf, M. Martinez-Velarte, M. Vrekoussis, R. Sussmann, I. Morino, K. Strong, et al. 2025. "Five Years of GOSAT-2 Retrievals with RemoTeC: XCO_2 and XCH_4 Data Products with Quality Filtering By Machine Learning." *Atmospheric Measurement Techniques* 18: 6093–6123. https://doi.org/10.5194/amt-18-6093-2025.

Blaustein-Rejto, D. and C. Gambino. 2023. *Livestock Don't Contribute 14.5% of Global Greenhouse Gas Emissions*. Oakland, CA: The Breakthrough Institute.

Bloom, A. A., P. I. Palmer, A. Fraser, D. S. Reay, and C. Frankenberg. 2010. "Large-Scale Controls of Methanogenesis Inferred from Methane and Gravity Spaceborne Data." *Science (New York, N.Y.)* 327: 322–325. https://doi.org/10.1126/science.1175176.

Butz, A., S. Guerlet, O. Hasekamp, D. Schepers, A. Galli, I. Aben, C. Frankenberg, et al. 2011. "Toward Accurate CO_2 and CH_4 Observations from Gosat." *Geophysical Research Letters* 38: 6–n/a. https://doi.org/10.1029/2011GL047888.

Chen, Z., D. J. Jacob, H. Nesser, M. P. Sulprizio, A. Lorente, D. J. Varon, X. Lu, et al. 2022. "Methane Emissions from China: A High-Resolution Inversion of TROPOMI Satellite Observations." *Atmospheric Chemistry and Physics* 22: 10809–10826. https://doi.org/10.5194/acp-22-10809-2022.

Chen, Z., D. J. Jacob, R. Gautam, M. Omara, R. N. Stavins, R. C. Stowe, H. Nesser, et al. 2023. "Satellite Quantification of Methane Emissions and Oil-Gas Methaneintensities from Individual Countries in the Middle East and North Africa: Implications for Climate Action." *Atmospheric Chemistry and Physics* 23: 5945–5967. https://doi.org/10.5194/acp-23-5945-2023.

Chen, Z., H. Lin, N. Balasus, A. Hardy, J. D. East, Y. Zhang, B. R. K. Runkle, et al. 2025. "Global Rice Paddy Inventory (GRPI): A High-Resolution Inventory of Methane Emissions from Rice Agriculture Based on Landsat Satellite Inundation Data." *Earth's Future* 13: e2024EF005479. https://doi.org/10.1029/2024EF005479.

Crippa, M., Guizzardi, D., Pagani, F., Banja, M., Muntean, M., Schaaf, E., Becker, W., Monforti-Ferrario, F., Quadrelli, R., and Risquez Martin, A. 2025) *GHG Emissions of All World Countries*. Luxembourg: Publications Office of the European Union. JRC143227.

Cusworth, D. H., A. K. Thorpe, A. K. Ayasse, D. Stepp, J. Heckler, G. P. Asner, C. E. Miller, V. Yadav, J. W. Chapman, and M. L. Eastwood. 2022. "Strong Methane Point Sources Contribute a Disproportionate Fraction of Total Emissions Across Multiple Basins in the United States." *Proceedings of the National Academy of Sciences of the United States of America* 119: e2202338119. https://doi.org/10.1073/pnas.2202338119.

Cusworth, D. H., D. J. Jacob, J. X. Sheng, J. Benmergui, A. J. Turner, J. Brandman, L. White, and C. A. Randles. 2018. "Detecting High-Emitting Methane Sources in Oil/Gas Fields Using Satellite Observations." *Atmospheric Chemistry and Physics* 18: 16885–16896. https://doi.org/10.5194/acp-18-16885-2018.

Cusworth, D. H., R. M. Duren, A. K. Thorpe, S. Pandey, J. D. Maasakkers, I. Aben, D. Jervis, et al. 2021b. "Multisatellite Imaging of a Gas Well Blowout Enables Quantification of Total Methane Emissions." *Geophysical Research Letters* 48: e2020GL090864. https://doi.org/10.1029/2020GL090864.

Cusworth, D. H., R. M. Duren, A. K. Thorpe, W. Olson-Duvall, J. Heckler, J. W. Chapman, M. L. Eastwood, et al. 2021a. "Intermittency of Large Methane Emitters in the Permian Basin." *Environmental Science & Technology Letters* 8: 567–573. https://doi.org/10.1021/acs.estlett.1c00173.

Cusworth, D. H., R. M. Duren, V. Yadav, A. K. Thorpe, K. Verhulst, S. Sander, F. Hopkins, T. Rafiq, and C. E. Miller. 2020. "Synthesis of Methane Observations Across Scales: Strategies for Deploying a Multitiered Observing Network." *Geophysical Research Letters* 47: 9. https://doi.org/10.1029/2020GL087869.

Dadheech, N., T. L. He, and A. J. Turner. 2025. "High-Resolution Greenhouse Gas Flux Inversions Using a Machine Learning Surrogate Model for Atmospheric Transport." *Atmospheric Chemistry and Physics* 25: 5159–5174. https://doi.org/10.5194/acp-25-5159-2025.

de Foy, B., J. J. Schauer, A. Lorente, and T. Borsdorff. 2023. "Investigating High Methane Emissions from Urban Areas Detected By TROPOMI and Their Association with Untreated Wastewater." *Environmental Research Letters*18: 21. https://doi.org/10.1088/1748-9326/acc118.

de Gouw, J. A., J. P. Veefkind, E. Roosenbrand, B. Dix, J. C. Lin, J. Landgraf, and P. F. Levelt. 2020. "Daily Satellite Observations of Methane from Oil and Gas Production Regions in the United States." *Science Reports* 10: 10. https://doi.org/10.1038/s41598-020-57678-4.

Dogniaux, M., J. D. Maasakkers, M. Girard, D. Jervis, J. McKeever, B. J. Schuit, S. Sharma, A. Lopez-Noreña, D. J. Varon, and I. Aben. 2025. "Global Satellite Survey Reveals Uncertainty in Landfill Methane Emissions." *Nature (London)* 647: 397–402. https://doi.org/10.1038/s41586-025-09683-8.

Duren, R., D. Cusworth, A. Ayasse, K. Howell, A. Diamond, T. Scarpelli, J. Kim, et al. 2025. "The Carbon Mapper Emissions Monitoring System." *EGUsphere* 2025: 1–41.

Duren, R. M., A. K. Thorpe, K. T. Foster, T. Rafiq, F. M. Hopkins, V. Yadav, B. D. Bue, et al. 2019. "California's Methane Super-Emitters." *Nature (London)* 575: 180–184. https://doi.org/10.1038/s41586-019-1720-3.

ESA. 2025. *European Space Agency*. https://sentinels.copernicus.eu/missions/sentinel-5/data-products

Estrada, L. A., D. J. Varon, M. Sulprizio, H. Nesser, Z. Chen, N. Balasus, S. E. Hancock, et al. 2025. "Integrated Methane Inversion (IMI) 2.0: An Improved Research and Stakeholder Tool for Monitoring Total Methane Emissions with High Resolution Worldwide Using TROPOMI Satellite Observations." *Geosci. Model Dev*. 18: 3311–3330. https://doi.org/10.5194/gmd-18-3311-2025.

European Commission and United States of America. 2021. Global methane pledge.

Frankenberg, C., U. Platt, and T. Wagner. 2005. "Iterative Maximum a Posteriori (IMAP)-DOAS for Retrieval of Strongly Absorbing Trace Gases: Model Studies for CH_4 and CO_2 Retrieval from Near Infrared Spectra of SCIAMACHY Onboard Envisat." *Atmospheric Chemistry and Physics* 5: 9–22. https://doi.org/10.5194/acp-5-9-2005.

Guanter, L., J. Roger, S. Sharma, A. Valverde, I. Irakulis-Loitxate, J. Gorrono, X. Zhang, et al. 2024. "Multisatellite Data Depicts a Record-Breaking Methane Leak from a Well Blowout." *Environmental Science & Technology Letters* 11: 825–830. https://doi.org/10.1021/acs.estlett.4c00399.

Hachmeister, J., O. Schneising, M. Buchwitz, A. Lorente, T. Borsdorff, J. P. Burrows, J. Notholt, and M. Buschmann. 2022. "On the Influence of Underlying Elevation Data on Sentinel-5 Precursor TROPOMI Satellite Methane Retrievals over Greenland." *Atmospheric Measurement Techniques* 15: 4063–4074. https://doi.org/10.5194/amt-15-4063-2022.

Hancock, S. E., D. J. Jacob, Z. Chen, H. Nesser, A. Davitt, D. J. Varon, M. P. Sulprizio, et al. 2025. "Satellite Quantification of Methane Emissions from South American Countries: A High-Resolution Inversion of TROPOMI and GOSAT Observations." *Atmospheric Chemistry and Physics* 25: 797–817. https://doi.org/10.5194/acp-25-797-2025.

Hari, M., R. K. Sahu, M. S. Sunder, and B. Tyagi. 2022. "Then and Now: COVID-19 Pandemic Lockdown Misfire Atmospheric Methane over India." *Aerosol and Air Quality Research* 22: 10. https://doi.org/10.4209/aaqr.210354.

Hasekamp, O. P., and A. Butz. 2008. "Efficient Calculation of Intensity and Polarization Spectra in Vertically Inhomogeneous Scattering and Absorbing Atmospheres." *J Geophys Res-Atmos* 113: 11. https://doi.org/10.1029/2008JD010379.

Hayashida, S., A. Ono, S. Yoshizaki, C. Frankenberg, W. Takeuchi, and X. Yan. 2013. "Methane Concentrations over Monsoon Asia as Observed By SCIAMACHY: Signals of Methane Emission from Rice Cultivation." *Remote Sensing of the Environment* 139: 246–256. https://doi.org/10.1016/j.rse.2013.08.008.

He, C., X. Lu, Y. Zhang, Z. Liu, F. Jiang, Y. Sun, M. Gao, et al. 2024. "Revisiting the Quantification of Power Plant CO_2 Emissions in the United States and China from Satellite: A Comparative Study Using Three Top-Down Approaches." *Remote Sensing of the Environment* 308: 114192. https://doi.org/10.1016/j.rse.2024.114192.

Helfter, C., M. Gondwe, M. Murray-Hudson, A. Makati, M. F. Lunt, P. I. Palmer, and U. Skiba. 2022. "Phenology Is the Dominant Control of Methane Emissions in a Tropical Non-Forested Wetland." *Nature Communications* 13: 133. https://doi.org/10.1038/s41467-021-27786-4.

Hemati, M., M. Mahdianpari, R. Nassar, H. Shiri, and F. Mohammadimanesh. 2024. "Urban Methane Emission Monitoring Across North America Using TROPOMI Data: An Analytical Inversion Approach." *Scientific Reports* 14: 9041. https://doi.org/10.1038/s41598-024-58995-8.

Hu, H., J. Landgraf, R. Detmers, T. Borsdorff, J. A. de Brugh, I. Aben, A. Butz, and O. Hasekamp. 2018. "Toward Global Mapping of Methane with TROPOMI: First Results and Intersatellite Comparison to Gosat." *Geophysical Research Letters* 45: 3682–3689. https://doi.org/10.1002/2018GL077259.

Hu, H., O. Hasekamp, A. Butz, A. Galli, J. Landgraf, J. Brugh, T. Borsdorff, R. Scheepmaker, and I. Aben. 2016. "The Operational Methane Retrieval Algorithm for Tropomi." *Atmospheric Measurement Techniques* 9: 5423–5440. https://doi.org/10.5194/amt-9-5423-2016.

Humpage, N., H. Boesch, W. Okello, J. Chen, F. Dietrich, M. F. Lunt, L. Feng, P. I. Palmer, and F. Hase. 2024. "Greenhouse Gas Column Observations from a Portable Spectrometer in Uganda." *Atmospheric Measurement Techniques* 17: 5679–5707. https://doi.org/10.5194/amt-17-5679-2024.

IPCC. 2023. *Climate Change 2021 – The Physical Science Basis: Working Group I Contribution to the Sixth Assessment Report of the Intergovernmental Panel on Climate Change*. Cambridge: Cambridge University.

Jacob, D. J., A. J. Turner, J. D. Maasakkers, J. X. Sheng, K. Sun, X. Liu, K. Chance, I. Aben, J. McKeever, and C. Frankenberg. 2016. "Satellite Observations of Atmospheric Methane and Their Value for Quantifying Methane Emissions." *Atmospheric Chemistry and Physics* 16: 14371–14396. https://doi.org/10.5194/acp-16-14371-2016.

Jacob, D. J., D. J. Varon, D. H. Cusworth, P. E. Dennison, C. Frankenberg, R. Gautam, L. Guanter, et al. 2022. "Quantifying Methane Emissions from the Global Scale down to Point Sources Using Satellite Observations of Atmospheric Methane." *Atmospheric Chemistry and Physics* 22: 9617–9646. https://doi.org/10.5194/acp-22-9617-2022.

Jensen, K., and K. McDonald. 2019. "Surface Water Microwave Product Series Version 3: A Near-Real Time and 25-Year Historical Global Inundated Area Fraction Time Series from Active and Passive Microwave Remote Sensing." *IEEE Geoscience and Remote Sensing Letters* 16: 1402–1406. https://doi.org/10.1109/LGRS.2019.2898779.

Jervis, D., J. McKeever, B. O. A. Durak, J. J. Sloan, D. Gains, D. J. Varon, A. Ramier, M. Strupler, and E. Tarrant. 2021. "The GHGSat-D Imaging Spectrometer." *Atmospheric Measurement Techniques* 14: 2127–2140. https://doi.org/10.5194/amt-14-2127-2021.

Jervis, D., M. Girard, J. P. MacLean, D. Marshall, J. McKeever, A. Ramier, M. Strupler, E. Tarrant, D. Young, and J. D. Maasakkers. 2025. “Global Energy Sector Methane Emissions Estimated By Using Facility-Level Satellite Observations.” *Science* 390: 1151–1155. https://10.1126/science.adv3183.

Jongaramrungruang, S., A. K. Thorpe, G. Matheou, and C. Frankenberg. 2022. “MethaNet - an AI-driven Approach to Quantifying Methane Point-Source Emission from High-Resolution 2-D Plume Imagery.” *Remote Sensing of the Environment* 269: 12. https://doi.org/10.1016/j.rse.2021.112809.

Karoff, C., and A. L. Vara-Vela. 2023. “Data Driven Analysis of Atmospheric Methane Concentrations as Function of Geographic, Land Cover Type and Season.” *Front. Earth Sci.* 11: 14. https://doi.org/10.3389/feart.2023.1119977.

Kenea, S. T., H. Y. Lee, S. W. Joo, S. L. Li, L. D. Labzovskii, C. Y. Chung, and Y. H. Kim. 2021. “Interannual Variability of Atmospheric CH_4 and Its Driver over South Korea Captured By Integrated Data in 2019.” *Remote Sensing* 13: 14. https://doi.org/10.3390/rs13122266.

Kozicka, K., D. Gozdowski, and E. Wojcik-Gront. 2021. “Spatial-Temporal Changes of Methane Content in the Atmosphere for Selected Countries and Regions with High Methane Emission from Rice Cultivation.” *Atmosphere* 12: 16. https://doi.org/10.3390/atmos12111382.

Kozicka, K., Z. Orazalina, D. Gozdowski, and E. Wójcik-Gront. 2023. “Evaluation of Temporal Changes in Methane Content in the Atmosphere for Areas with a Very High Rice Concentration Based on Sentinel-5P Data.” *Remote Sensing Applications: Society and Environment* 30: 100972. https://doi.org/10.1016/j.rsase.2023.100972.

Krings, T., K. Gerilowski, M. Buchwitz, M. Reuter, A. Tretner, J. Erzinger, D. Heinze, U. Pfluger, J. P. Burrows, and H. Bovensmann. 2011. “MAMAP—a New Spectrometer System for Column-Averaged Methane and Carbon Dioxide Observations from Aircraft: Retrieval Algorithm and First Inversions for Point Source Emission Rates.” *Atmospheric Measurement Techniques* 4: 1735–1758. https://doi.org/10.5194/amt-4-1735-2011.

Lambert, J., Compernolle, S., Eichmann, K., de Graaf, M., Hubert, D., Keppens, A., Kleipool, Q., Langerock, B., Sha, M., and Verhoelst, T. 2025.*S5P MPC Routine Operations Consolidated Validation Report Series*. Version 28, 227.

Lauvaux, T., C. Giron, M. Mazzolini, A. d'Aspremont, R. Duren, D. Cusworth, D. Shindell, and P. Ciais. 2022. “Global Assessment of Oil and Gas Methane Ultra-Emitters.” *Science (New York, N.Y.)* 375: 557–561. https://doi.org/10.1126/science.abj4351.

Li, F., S. X. Bai, K. R. Lin, C. X. Feng, S. W. Sun, S. H. Zhao, Z. T. Wang, W. Zhou, C. Y. Zhou, and Y. G. Zhang. 2024a. “Satellite-Based Surveys Reveal Substantial Methane Point-Source Emissions in Major Oil & Gas Basins of North America during 2022-2023.” *Journal of Geophysical Research: Atmosphere* 129: e2024JD040870.

Li, M., E. A. Kort, A. A. Bloom, D. Wu, G. Plant, C. Gerlein-Safdi, and T. J. E. S. Pu. 2024b. “Underestimated Dry Season Methane Emissions from Wetlands in the Pantanal.” *Technology* 58: 3278–3287.

Li, S. W., C. B. Wang, P. Y. Gao, B. J. Zhao, C. L. Jin, L. Zhao, B. T. He, and Y. Xue. 2023. “High-Spatial-Resolution Methane Emissions Calculation Using TROPOMI Data By a Divergence Method.” *Atmosphere* 14: 13. https://doi.org/10.3390/atmos14020388.

Liang, R., Y. Zhang, Q. Hu, T. Li, S. Li, W. Yuan, J. Xu, et al. 2024. “Satellite-Based Monitoring of Methane Emissions from China's Rice Hub.” *Environmental Science & Technology* 58: 23127–23137. https://doi.org/10.1021/acs.est.4c09822.

Liang, R., Y. Zhang, W. Chen, P. Zhang, J. Liu, C. Chen, H. Mao, et al. 2023. “East Asian Methane Emissions Inferred from High-Resolution Inversions of GOSAT and TROPOMI Observations: A Comparative and Evaluative Analysis.” *Atmospheric Chemistry and Physics* 23: 8039–8057. https://doi.org/10.5194/acp-23-8039-2023.

Lin, X., S. Peng, P. Ciais, D. Hauglustaine, X. Lan, G. Liu, M. Ramonet, et al. 2024. “Recent Methane Surges Reveal Heightened Emissions from Tropical Inundated Areas.” *Nature Communications* 15: 10894. https://doi.org/10.1038/s41467-024-55266-y.

Lindqvist, H., E. Kivimäki, T. Häkkilä, A. Tsuruta, O. Schneising, M. Buchwitz, A. Lorente, et al. 2024. “Evaluation of Sentinel-5P TROPOMI Methane Observations at Northern High Latitudes.” *Remote Sensing* 16: 2979. https://doi.org/10.3390/rs16162979.

Liu, L., L. Chen, Y. Liu, D. Yang, X. Zhang, N. Lu, W. Ju, F. Jiang, Z. Yin, and G. Liu. 2022. “Satellite Remote Sensing for Global Stocktaking: Methods, Progress and Perspectives.” *National Remote Sensing Bulletin* 26: 243–267. https://doi.org/10.11834/jrs.20221806.

Liu, M., A. R. van der, M. van Weele, L. Bryan, H. Eskes, P. Veefkind, Y. Liu, X. Lin, J. de Laat, and J. Ding. 2024. “Current Potential of CH_4 Emission Estimates Using TROPOMI in the Middle East.” *EGUsphere* 2024: 1–29.

Liu, M. Y., R. van der A, M. van Weele, H. Eskes, X. Lu, P. Veefkind, J. de Laat, et al. 2021a. “A New Divergence Method to Quantify Methane Emissions Using Observations of Sentinel-5P Tropomi.” *Geophysical Research Letters* 48: 10. https://doi.org/10.1029/2021GL094151.

Liu, Y., J. Wang, K. Che, Z. Cai, D. Yang, and L. Wu. 2021b. “Satellite Remote Sensing of Greenhouse Gases: Progress and Trends.” *National Remote Sensing Bulletin* 26: 243–267.

Lorente, A., T. Borsdorff, A. Butz, O. Hasekamp, J. aan de Brugh, A. Schneider, L. H. Wu, et al. 2021. “Methane Retrieved from TROPOMI: Improvement of the Data Product and Validation of the First 2 Years of Measurements.” *Atmospheric Measurement Techniques* 14: 665–684. https://doi.org/10.5194/amt-14-665-2021.

Lorente, A., T. Borsdorff, M. C. Martinez-Velarte, and J. Landgraf. 2023. “Accounting for Surface Reflectance Spectral Features in TROPOMI Methane Retrievals.” *Atmospheric Measurement Techniques* 16: 1597–1608. https://doi.org/10.5194/amt-16-1597-2023.

Lu, X., D. J. Jacob, H. L. Wang, J. D. Maasakkers, Y. Z. Zhang, T. R. Scarpelli, L. Shen, et al. 2022. "Methane Emissions in the United States, Canada, and Mexico: Evaluation of National Methane Emission Inventories and 2010-2017 Sectoral Trends By Inverse Analysis of in Situ (GLOBALVIEWplus CH_4 ObsPack) and Satellite (GOSAT) Atmospheric Observations." *Atmospheric Chemistry and Physics* 22: 395–418. https://doi.org/10.5194/acp-22-395-2022.

Maasakkers, J. D., D. J. Varon, A. Elfarsdottir, J. McKeever, D. Jervis, G. Mahapatra, S. Pandey, et al. 2022b. "Using Satellites to Uncover Large Methane Emissions from Landfills." *Science Advances* 8: 9. https://doi.org/10.1126/sciadv.abn9683.

Maasakkers, J. D., M. Omara, R. Gautam, A. Lorente, S. Pandey, P. Tol, T. Borsdorff, S. Houweling, and I. Aben. 2022a. "Reconstructing and Quantifying Methane Emissions from the Full Duration of a 38-Day Natural Gas Well Blowout Using Space-Based Observations." *Remote Sensing of the Environment* 270: 7. https://doi.org/10.1016/j.rse.2021.112755.

Mazzini, A., A. Sciarra, G. Etiope, P. Sadavarte, S. Houweling, S. Pandey, and A. Husein. 2021. "Relevant Methane Emission to the Atmosphere from a Geological Gas Manifestation." *Science Reports* 11: 10. https://doi.org/10.1038/s41598-021-83369-9.

McLinden, C. A., D. Griffin, Z. Davis, C. Hempel, J. Smith, C. Sioris, R. Nassar, O. Moeini, E. Legault-Ouellet, and A. Malo. 2024. "An Independent Evaluation of GHGSat Methane Emissions: Performance Assessment." *Journal of Geophysical Research: Atmospheres* 129: e2023JD039906. https://doi.org/10.1029/2023JD039906.

Mermigkas, M., C. Topaloglou, D. Balis, M. E. Koukouli, F. Hase, D. Dubravica, T. Borsdorff, and A. Lorente. 2021. "FTIR Measurements of Greenhouse Gases over Thessaloniki, Greece in the Framework of COCCON and Comparison with S5P/TROPOMI Observations." *Remote Sensing* 13: 21. https://doi.org/10.3390/rs13173395.

Mohammadimanesh, F., M. Mahdianpari, A. Radman, D. Varon, M. Hemati, and M. Marjani. 2025. "Advancements in Satellite-Based Methane Point Source Monitoring: A Systematic Review." *ISPRS Journal of Photogrammetry and Remote Sensing* 224: 94–112. https://doi.org/10.1016/j.isprsjprs.2025.03.020.

Nathan, B., J. D. Maasakkers, S. Naus, R. Gautam, M. Omara, D. J. Varon, M. P. Sulprizio, et al. 2024. "Assessing Methane Emissions from Collapsing Venezuelan Oil Production Using Tropomi." *Atmospheric Chemistry and Physics* 24: 6845–6863. https://doi.org/10.5194/acp-24-6845-2024.

Nepstad, L. S., J. S. Gerber, J. D. Hill, L. C. P. Dias, M. H. Costa, and P. C. West. 2019. "Pathways for Recent Cerrado Soybean Expansion: Extending the Soy Moratorium and Implementing Integrated Crop Livestock Systems with Soybeans." *Environmental Research Letters*14: 14. https://doi.org/10.1088/1748-9326/aafb85.

Nesme, N., R. Marion, O. Lezeaux, S. Doz, C. Camy-Peyret, and P. Y. Foucher. 2021. "Joint Use of In-Scene Background Radiance Estimation and Optimal Estimation Methods for Quantifying Methane Emissions Using PRISMA Hyperspectral Satellite Data: Application to the Korpezhe Industrial Site." *Remote Sensing* 13: 4992. https://doi.org/10.3390/rs13244992.

Nesser, H., D. J. Jacob, J. D. Maasakkers, A. Lorente, Z. Chen, X. Lu, L. Shen, et al. 2024. "High-Resolution US Methane Emissions Inferred from an Inversion of 2019 TROPOMI Satellite Data: Contributions from Individual States, Urban Areas, and Landfills." *Atmospheric Chemistry and Physics* 24: 5069–5091. https://doi.org/10.5194/acp-24-5069-2024.

Nisbet, E. G., E. J. Dlugokencky, M. R. Manning, D. Lowry, R. E. Fisher, J. L. France, S. E. Michel, et al. 2016. "Rising Atmospheric Methane: 2007-2014 Growth and Isotopic Shift." *Global Biogeochemical Cycles*30: 1356–1370. https://doi.org/10.1002/2016GB005406.

Nisbet, E. G., M. R. Manning, E. J. Dlugokencky, R. E. Fisher, D. Lowry, S. E. Michel, C. L. Myhre, et al. 2019. "Very Strong. Atmospheric Methane Growth in the 4 Years 2014-2017: Implications for the Paris Agreement." *Global Biogeochemical Cycles* 33: 318–342. https://doi.org/10.1029/2018GB006009.

Pandey, S., M. van Nistelrooij, J. D. Maasakkers, P. Sutar, S. Houweling, D. J. Varon, P. Tol, D. Gains, J. Worden, and I. Aben. 2023. "Daily Detection and Quantification of Methane Leaks Using Sentinel-3: A Tiered Satellite Observation Approach with Sentinel-2 and Sentinel-5P." *Remote Sensing of Environment* 296: 113716. https://doi.org/10.1016/j.rse.2023.113716.

Pandey, S., R. Gautam, S. Houweling, H. D. van der Gon, P. Sadavarte, T. Borsdorff, O. Hasekamp, et al. 2019. "Satellite Observations Reveal Extreme Methane Leakage from a Natural Gas Well Blowout." *Proceedings of the National Academy of Science of The United States of America* 116: 26376–26381. https://doi.org/10.1073/pnas.1908712116.

Pandey, S., S. Houweling, A. Lorente, T. Borsdorff, M. Tsivlidou, A. A. Bloom, B. Poulter, Z. Zhang, and I. Aben. 2021. "Using Satellite Data to Identify the Methane Emission Controls of South Sudan's Wetlands." *Biogeosciences* 18: 557–572. https://doi.org/10.5194/bg-18-557-2021.

Park, H., S. Jeong, M. K. Sha, J. Lee, and M. M. Frey. 2024. "Comparisons of Greenhouse Gas Observation Satellite Performances over Seoul Using a Portable Ground-Based Spectrometer." *Geophysical Research Letters* 51: e2024GL109334. https://doi.org/10.1029/2024GL109334.

Parker, R. J., A. Webb, H. Boesch, P. Somkuti, R. Barrio Guillo, A. Di Noia, N. Kalaitzi, et al. 2020. "A Decade of GOSAT Proxy Satellite CH_4 Observations." *Earth System Science Data* 12: 3383–3412. https://doi.org/10.5194/essd-12-3383-2020.

Peng, S., C. Giron, G. Liu, A. d'Aspremont, A. Benoit, T. Lauvaux, X. Lin, H. d. A. Rodrigues, M. Saunois, and P. Ciais. 2023. "High-Resolution Assessment of Coal Mining Methane Emissions By Satellite in Shanxi, China." *Iscience* 26: 108375. https://doi.org/10.1016/j.isci.2023.108375.

Plant, G., E. A. Kort, L. T. Murray, J. D. Maasakkers, and I. Aben. 2022. "Evaluating Urban Methane Emissions from Space Using TROPOMI Methane and Carbon Monoxide Observations." *Remote Sensing of Environment* 268: 112756. https://doi.org/10.1016/j.rse.2021.112756.

Pollard, D. F. F., F. Hase, M. K. Sha, D. Dubravica, C. Alberti, and D. Smale. 2022. "Retrievals of X-CO_2, X-CH_4 and X-CO from Portable, Near-Infrared Fourier Transform Spectrometer Solar Observations in Antarctica." *Earth System Science Data* 14: 5427–5437. https://doi.org/10.5194/essd-14-5427-2022.

Puliafito, S. E., T. R. Bolano-Ortiz, L. Berna, and R. M. Pascual-Flores. 2020. "High Resolution Inventory of Atmospheric Emissions from Livestock Production, Agriculture, and Biomass Burning Sectors of Argentina." *Atmospheric Environment* 223: 14. https://doi.org/10.1016/j.atmosenv.2019.117248.

Qu, Z., D. J. Jacob, L. Shen, X. Lu, Y. Z. Zhang, T. R. Scarpelli, H. Nesser, et al. 2021. "Global Distribution of Methane Emissions: A Comparative Inverse Analysis of Observations from the TROPOMI and GOSAT Satellite Instruments." *Atmospheric Chemistry and Physics* 21: 14159–14175. https://doi.org/10.5194/acp-21-14159-2021.

Reuter, M., M. Buchwitz, O. Schneising, S. Noeel, H. Bovensmann, J. P. Burrows, H. Boesch, et al. 2020. "Ensemble-Based Satellite-Derived Carbon Dioxide and Methane Column-Averaged Dry-Air Mole Fraction Data Sets (2003-2018) for Carbon and Climate Applications." *Atmospheric Measurement Techniques* 13: 789–819. https://doi.org/10.5194/amt-13-789-2020.

Roberts, C., O. Shorttle, K. Mandel, M. Jones, R. Ijzermans, B. Hirst, and P. Jonathan. 2022. "Enhanced Monitoring of Atmospheric Methane from Space over the Permian Basin with Hierarchical Bayesian Inference." *Environmental Research Letters*17: 064037. https://doi.org/10.1088/1748-9326/ac7062.

Roberts, C., R. Ijzermans, D. Randell, M. Jones, P. Jonathan, K. Mandel, B. Hirst, and O. Shorttle. 2023. "Avoiding Methane Emission Rate Underestimates When Using the Divergence Method." *Environmental Research Letters*18: 114033. https://doi.org/10.1088/1748-9326/ad0252.

Roger, J., I. Irakulis-Loitxate, A. Valverde, J. Gorroño, S. Chabrillat, M. Brell, and L. Guanter. 2024. "High-Resolution Methane Mapping with the EnMAP Satellite Imaging Spectroscopy Mission." *IEEE Transactions on Geoscience and Remote Sensing PP* 62: 1–1. https://doi.org/10.1109/TGRS.2024.3352403.

Sadavarte, P., S. Pandey, J. D. Maasakkers, A. Lorente, T. Borsdorff, H. D. van der Gon, S. Houweling, and I. Aben. 2021. "Methane Emissions from Superemitting Coal Mines in Australia Quantified Using TROPOMI Satellite Observations." *Environmental Science & Technology* 55: 16573–16580. https://doi.org/10.1021/acs.est.1c03976.

Saunois, M., A. Martinez, B. Poulter, Z. Zhang, P. A. Raymond, P. Regnier, J. G. Canadell, et al. 2025. "Global Methane Budget 2000&Ndash2020." *Earth System Science Data* 17: 1873–1958. https://doi.org/10.5194/essd-17-1873-2025.

Schissel, C., and D. T. Allen. 2022. "Impact of the High-Emission Event Duration and Sampling Frequency on the Uncertainty in Emission Estimates." *Environmental Science & Technology Letters* 9: 1063–1067. https://doi.org/10.1021/acs.estlett.2c00731.

Schneider, M., B. Ertl, Q. Tu, C. J. Diekmann, F. Khosrawi, A. N. Roehling, F. Hase, et al. 2022. "Synergetic Use of IASI Profile and TROPOMI Total-Column Level 2 Methane Retrieval Products." *Atmospheric Measurement Techniques* 15: 4339–4371. https://doi.org/10.5194/amt-15-4339-2022.

Schneising, O., H. Bovensmann, M. Buchwitz, M. Buschmann, N. M. Deutscher, D. W. T. Griffith, J. Hachmeister, et al. 2025. "TROPOMI/WFMD v2.0: Improved Retrievals of XCH_4 and XCO with XGBoost-based Quality Filtering." *EGUsphere* 2025: 1–39.

Schneising, O., M. Buchwitz, J. Hachmeister, S. Vanselow, M. Reuter, M. Buschmann, H. Bovensmann, and J. P. Burrows. 2023. "Advances in Retrieving XCH_4 and XCO from Sentinel-5 Precursor: Improvements in the Scientific TROPOMI/WFMD Algorithm." *Atmospheric Measurement Techniques* 16: 669–694. https://doi.org/10.5194/amt-16-669-2023.

Schneising, O., M. Buchwitz, M. Reuter, H. Bovensmann, J. P. Burrows, T. Borsdorff, N. M. Deutscher, et al. 2019. "A Scientific Algorithm to Simultaneously Retrieve Carbon Monoxide and Methane from TROPOMI Onboard Sentinel-5 Precursor." *Atmospheric Measurement Techniques* 12: 6771–6802. https://doi.org/10.5194/amt-12-6771-2019.

Schneising, O., M. Buchwitz, M. Reuter, S. Vanselow, H. Bovensmann, and J. P. Burrows. 2020. "Remote Sensing of Methane Leakage from Natural Gas and Petroleum Systems Revisited." *Atmospheric Chemistry and Physics* 20: 9169–9182. https://doi.org/10.5194/acp-20-9169-2020.

Schuit, B. J., J. D. Maasakkers, P. Bijl, G. Mahapatra, A. W. van den Berg, S. Pandey, A. Lorente, et al. 2023. "Automated Detection and Monitoring of Methane Super-Emitters Using Satellite Data." *Atmospheric Chemistry and Physics* 23: 9071–9098. https://doi.org/10.5194/acp-23-9071-2023.

Settembre, D., D. De Santis, G. Schiavon, and F. Del Frate. 2025. "Methane Column Estimation Using PRISMA Hyperspectral Data and Comparison with Other Earth Observation Products." *IEEE Geoscience and Remote Sensing Letters* 22: 1–5. https://doi.org/10.1109/LGRS.2025.3539870.

Sha, M. K., B. Langerock, J. F. L. Blavier, T. Blumenstock, T. Borsdorff, M. Buschmann, A. Dehn, et al. 2021. "Validation of Methane and Carbon Monoxide from Sentinel-5 Precursor Using TCCON and NDACC-IRWG Stations." *Atmospheric Measurement Techniques* 14: 6249–6304. https://doi.org/10.5194/amt-14-6249-2021.

Shahzadi, K., M. Schneider, N. Ying Lo, F. Hase, J. Meyer, U. Cayoglu, T. Borsdorff, and M. C. Martinez-Velarte. 2025. "A Multi-Year Global Methane Data Set Obtained By Merging Observations from TROPOMI and IASI." *Earth System Science Data Discuss.* 2025: 1–31.

Shen, L., D. J. Jacob, R. Gautam, M. Omara, T. R. Scarpelli, A. Lorente, D. Zavala-Araiza, X. Lu, Z. Chen, and J. Lin. 2023. "National Quantifications of Methane Emissions from Fuel Exploitation Using High Resolution Inversions of Satellite Observations." *Nature Communications* 14: 4948. https://doi.org/10.1038/s41467-023-40671-6.

Shen, L., D. Zavala-Araiza, R. Gautam, M. Omara, T. Scarpelli, J. X. Sheng, M. P. Sulprizio, et al. 2021. "Unravelling a Large Methane Emission Discrepancy in Mexico Using Satellite Observations." *Remote Sensing of the Environment* 260: 9. https://doi.org/10.1016/j.rse.2021.112461.

Shen, L., R. Gautam, M. Omara, D. Zavala-Araiza, J. D. Maasakkers, T. R. Scarpelli, A. Lorente, et al. 2022. "Satellite Quantification of Oil and Natural Gas Methane Emissions in the US and Canada Including Contributions from Individual Basins." *Atmospheric Chemistry and Physics* 22: 11203–11215. https://doi.org/10.5194/acp-22-11203-2022.

Sheng, J. X., S. J. Song, Y. Z. Zhang, R. G. Prinn, and G. Janssens-Maenhout. 2019. "Bottom-Up Estimates of Coal Mine Methane Emissions in China: A Gridded Inventory, Emission Factors, and Trends." *Environmental Science & Technology Letters* 6: 473–478. https://doi.org/10.1021/acs.estlett.9b00294.

Sicsik-Paré, A., A. Fortems-Cheiney, I. Pison, G. Broquet, A. Opler, E. Potier, A. Martinez, et al. 2025. "Can We Obtain Consistent Estimates of the Emissions in Europe from Three Different CH_4 TROPOMI Products?." *EGUsphere* 2025: 1–48.

Somkuti, P., G. McGarragh, C. O'Dell, A. Di Noia, L. Vogel, S. Crowell, L. E. Ott, and H. Bösch. 2025. "Surface Reflectance Biases in XCH_4 Retrievals from the 2.3 µm Band Are Enhanced in the Presence of Aerosols." *Atmospheric Measurement Techniques* 18: 4647–4663. https://doi.org/10.5194/amt-18-4647-2025.

Suthar, G., S. Singh, N. Kaul, and S. Khandelwal. 2024. "Analyzing Methane Emissions in Five Indian Cities Using TROPOMI Data from sentinel-5 Precursor Satellite." *Urban Climate* 58: 102174. https://doi.org/10.1016/j.uclim.2024.102174.

Tang, G., Y. Zhang, W. Chen, Z. Luo, J. Maasakkers, and J. Worden. 2025. "Satellite Methane and Ammonia Observations Consistently Show Substantial Increases in Pan-Tropical Livestock Emissions." *Environmental Research Letters* 20: 114005. https://doi.org/10.1088/1748-9326/ae0955.

Tanimoto, H., T. Matsunaga, Y. Someya, T. Fujinawa, H. Ohyama, I. Morino, H. Yashiro, et al. 2025. "The Greenhouse Gas Observation Mission with Global Observing SATellite for Greenhouse Gases and Water Cycle (GOSAT-GW): Objectives, Conceptual Framework and Scientific Contributions." *Progress in Earth and Planetary Science* 12: 8.

Tsuruta, A., E. Kivimäki, H. Lindqvist, T. Karppinen, L. Backman, J. Hakkarainen, O. Schneising, et al. 2023. "CH_4 Fluxes Derived from Assimilation of TROPOMI XCH_4 in CarbonTracker Europe-CH_4: Evaluation of Seasonality and Spatial Distribution in the Northern High Latitudes." *Remote Sensing* 15: 1620. https://doi.org/10.3390/rs15061620.

Tu, Q., F. Hase, M. Schneider, O. Garcia, T. Blumenstock, T. Borsdorff, M. Frey, et al. 2022a. "Quantification of CH_4 Emissions from Waste Disposal Sites Near the City of Madrid Using ground- and Space-Based Observations of COCCON, TROPOMI and Iasi." *Atmospheric Chemistry and Physics* 22: 295–317. https://doi.org/10.5194/acp-22-295-2022.

Tu, Q. S., F. Hase, M. Schneider, O. Garcia, T. Blumenstock, T. Borsdorff, M. Frey, et al. 2022b. "Quantification of CH_4 Emissions from Waste Disposal Sites Near the City of Madrid Using ground- and Space-Based Observations of COCCON, TROPOMI and Iasi." *Atmospheric Chemistry and Physics* 22: 295–317. https://doi.org/10.5194/acp-22-295-2022.

Tu, Q. S., F. Hase, K. Qin, C. Alberti, F. Lu, Z. Bian, L. X. Cao, et al. 2024. "COCCON Measurements of XCO_2, XCH_4 and XCO over Coal Mine Aggregation Areas in Shanxi, China, and Comparison to TROPOMI and CAMS Datasets." *Remote Sensing* 16: 4022. https://doi.org/10.3390/rs16214022.

Tu, Q. S., M. Schneider, F. Hase, F. Khosrawi, B. Ertl, J. Necki, D. Dubravica, C. J. Diekmann, T. Blumenstock, and D. J. Fang. 2022c. "Quantifying CH_4 Emissions in Hard Coal Mines from TROPOMI and IASI Observations Using the Wind-Assigned Anomaly Method." *Atmospheric Chemistry and Physics* 22: 9747–9765. https://doi.org/10.5194/acp-22-9747-2022.

Vanselow, S., O. Schneising, M. Buchwitz, M. Reuter, H. Bovensmann, H. Boesch, and J. P. Burrows. 2024. "Automated Detection of Regions with Persistently Enhanced Methane Concentrations Using Sentinel-5 Precursor Satellite Data." *Atmospheric Chemistry and Physics* 24: 10441–10473. https://doi.org/10.5194/acp-24-10441-2024.

Vara-Vela, A. L., N. R. Benavente, O. K. Nielsen, J. P. Nascimento, R. Alves, M. Gavidia-Calderon, and C. Karoff. 2024. "Quantifying Methane Emissions Using Satellite Data: Application of the Integrated Methane Inversion (IMI) Model to Assess Danish Emissions." *Remote Sensing* 16: 4554. https://doi.org/10.3390/rs16234554.

Varon, D. J., D. J. Jacob, J. McKeever, D. Jervis, B. O. A. Durak, Y. Xia, and Y. Huang. 2018. "Quantifying Methane Point Sources from Fine-Scale Satellite Observations of Atmospheric Methane Plumes." *Atmospheric Measurement Techniques* 11: 5673–5686. https://doi.org/10.5194/amt-11-5673-2018.

Varon, D. J., D. J. Jacob, B. Hmiel, R. Gautam, D. R. Lyon, M. Omara, M. Sulprizio, et al. 2023. "Continuous Weekly Monitoring of Methane Emissions from the Permian Basin By Inversion of TROPOMI Satellite Observations." *Atmospheric Chemistry and Physics* 23: 7503–7520. https://doi.org/10.5194/acp-23-7503-2023.

Varon, D. J., D. Jervis, J. McKeever, I. Spence, D. Gains, and D. J. Jacob. 2021. "High-Frequency Monitoring of Anomalous Methane Point Sources with Multispectral Sentinel-2 Satellite Observations." *Atmospheric Measurement Techniques* 14: 2771–2785. https://doi.org/10.5194/amt-14-2771-2021.

Varon, D. J., D. J. Jacob, M. Sulprizio, L. A. Estrada, W. B. Downs, L. Shen, S. E. Hancock, et al. 2022. "Integrated Methane Inversion (IMI 1.0): A User-Friendly, Cloud-Based Facility for Inferring High-Resolution Methane Emissions from TROPOMI Satellite Observations." *Geoscientific Model Development* 15: 5787–5805. https://doi.org/10.5194/gmd-15-5787-2022.

Veefkind, J. P., I. Aben, K. McMullan, H. Förster, J. de Vries, G. Otter, J. Claas, et al. 2012. "TROPOMI on the ESA Sentinel-5 Precursor: A GMES Mission for Global Observations of the Atmospheric Composition for Climate, Air Quality and Ozone Layer Applications." *Remote Sensing of the Environment* 120: 70–83. https://doi.org/10.1016/j.rse.2011.09.027.

Veefkind, J. P., R. Serrano-Calvo, J. de Gouw, B. Dix, O. Schneising, M. Buchwitz, J. Barré, R. J. van der A, M. Liu, and P. F. Levelt. 2023. "Widespread Frequent Methane Emissions from the Oil and Gas Industry in the Permian Basin." *Journal of Geophysical Research: Atmospheres* 128: e2022JD037479. https://doi.org/10.1029/2022JD037479.

Ward, R. H., L. M. Western, R. L. Tunnicliffe, E. Fillola, A. Tsuruta, T. Aalto, and A. L. Ganesan. 2025. "Uncertainty and Retrieval Sensitivity in TROPOMI-based Methane Inversions over the North Slope of Alaska." *EGUsphere* 2025: 1–38.

Wang, Y. C., X. Guo, Y. J. Huo, M. Y. Li, Y. Q. Pan, S. C. Yu, A. Baklanov, D. Rosenfeld, J. H. Seinfeld, and P. F. Li. 2023. "Toward a Versatile Spaceborne Architecture for Immediate Monitoring of the Global Methane Pledge." *Atmospheric Chemistry and Physics* 23: 5233–5249. https://doi.org/10.5194/acp-23-5233-2023.

Worden, J. R., D. H. Cusworth, Z. Qu, Y. Yin, Y. Zhang, A. A. Bloom, S. Ma, et al. 2022. "The 2019 Methane Budget and Uncertainties at 1° Resolution and Each Country through Bayesian Integration of GOSAT Total Column Methane Data and a Priori Inventory Estimates." *Atmospheric Chemistry and Physics* 22: 6811–6841. https://doi.org/10.5194/acp-22-6811-2022.

Wunch, D., G. C. Toon, J.-F. L. Blavier, R. A. Washenfelder, J. Notholt, B. J. Connor, D. W. T. Griffith, V. Sherlock, and P. O. Wennberg. 2011. "The Total Carbon Column Observing Network." *Philosophical Transactions of the Royal Society A: Mathematical, Physical and Engineering Sciences* 369: 2087–2112. https://doi.org/10.1098/rsta.2010.0240.

Yu, X. Y., D. B. Millet, D. K. Henze, A. J. Turner, A. L. Delgado, A. A. Bloom, and J. X. Sheng. 2023. "A High-Resolution Satellite-Based Map of Global Methane Emissions Reveals Missing Wetland, Fossil Fuel, and Monsoon Sources." *Atmospheric Chemistry and Physics* 23: 3325–3346. https://doi.org/10.5194/acp-23-3325-2023.

Zavala-Araiza, D., M. Omara, R. Gautam, M. L. Smith, S. Pandey, I. Aben, V. Almanza-Veloz, et al. 2021. "A Tale of Two Regions: Methane Emissions from Oil and Gas Production in Offshore/Onshore Mexico." *Environmental Research Letters*16: 11. https://doi.org/10.1088/1748-9326/abceeb.

Zhang, J. X., G. Han, H. Q. Mao, Z. P. Pei, X. Ma, W. J. Jia, and W. Gong. 2022. "The Spatial and Temporal Distribution Patterns of XCH_4 in China: New Observations from Tropomi." *Atmosphere* 13: 14. https://doi.org/10.3390/atmos13020177.

Zhang, Y. Z., D. J. Jacob, X. Lu, J. D. Maasakkers, T. R. Scarpelli, J. X. Sheng, L. Shen, et al. 2021. "Attribution of the Accelerating Increase in Atmospheric Methane during 2010-2018 By Inverse Analysis of GOSAT Observations." *Atmospheric Chemistry and Physics* 21: 3643–3666. https://doi.org/10.5194/acp-21-3643-2021.

Zhang, Y. Z., R. Gautam, S. Pandey, M. Omara, J. D. Maasakkers, P. Sadavarte, D. Lyon, et al. 2020. "Quantifying Methane Emissions from the Largest Oil-Producing Basin in the United States from Space." *Science Advances* 6: 9. https://doi.org/10.1126/sciadv.aaz5120.

Zhang, Z., B. Poulter, A. F. Feldman, Q. Ying, P. Ciais, S. Peng, and X. Li. 2023. "Recent Intensification of Wetland Methane Feedback." *Nature Climate Change* 13: 430–433. https://doi.org/10.1038/s41558-023-01629-0.

Zhong, H., L. Shen, M. Qu, Y. Ou, Y. Zhang, and H. Mao. 2025. "Quantifying Methane Emission Baselines with High-Resolution Satellite Data to Support China's Emission Control." *Science Bulletin* 70: 2255–2259. https://doi.org/10.1016/j.scib.2025.04.047.